

October 8, 1976

GAI REPORT NO. 1848

AN ANALYSIS OF LOW TRAJECTORY
TURBINE MISSILE HAZARD

to the

PERRY NUCLEAR POWER PLANT
UNITS 1 & 2

CLEVELAND ELECTRIC ILLUMINATING CO.
CLEVELAND, OHIO

Kenneth E. Weise

Stephen W. Webb

Jacquelyn Tate

Gilbert Associates, Inc.
525 Lancaster Avenue
Reading, Pennsylvania

TABLE OF CONTENTS

<u>Section</u>	<u>Title</u>	<u>Page</u>
1.0	<u>INTRODUCTION</u>	1
2.0	<u>GENERAL DESCRIPTION</u>	3
2.1	DESCRIPTION OF THE PERRY NUCLEAR POWER PLANT	3
2.2	LOW TRAJECTORY MISSILE TARGET ZONE	7
2.3	POSTULATED METHODS FOR COMPROMISING UNIT SAFETY	8
2.4	TURBINE MISSILE CHARACTERISTICS	9
3.0	<u>EVALUATION OF TURBINE MISSILE DAMAGE PROBABILITY</u>	10
3.1	INTRODUCTION	10
3.2	ANNUAL MISSILE EJECTION PROBABILITY - P_1	11
3.3	LTM STRIKE PROBABILITIES - P_2	12
3.3.1	<u>Method</u>	12
3.3.2	<u>LTM Strike Probabilities</u>	13
3.4	DAMAGE PREDICTION - P_3	14
3.4.1	<u>Method</u>	14
3.4.2	<u>Intermediate Barrier Interaction</u>	15
3.4.3	<u>Final Barriers</u>	21
3.4.4	<u>Missile Impact Parameters</u>	22
3.4.5	<u>Multiple Impacts</u>	25
3.4.6	<u>Statistics</u>	27
3.4.7	<u>Damage Probability</u>	29
3.5	TARGET DAMAGE PROBABILITIES - P_4	32
3.6	CONCLUSION	33
	REFERENCES	34

APPENDIX A RESIDUAL PERFORATION VELOCITY

APPENDIX B

LIST OF TABLES

2-1	SAFETY CLASSIFICATION AND LOCATION OF STRUCTURES
2-2	PROTECTIVE BARRIERS FOR LTM STRIKE TARGETS
2-3	SUMMARY OF DAMAGE MECHANISMS FOR COMPROMISING UNIT SAFETY
2-4	49 INCH LAST STAGE BUCKET - LP TURBINE - MISSILE CHARACTERISTICS
3-1	LTM STRIKE PROBABILITIES
3-2	LOWER AND UPPER IMPACT AREAS
3-3	P_3 DAMAGE PROBABILITIES FOR SINGLE IMPACT DESTRUCTIVE OVERSPEED
3-4	P_3 DAMAGE PROBABILITIES FOR DOUBLE IMPACT DESTRUCTIVE OVERSPEED
3-5	P_3 DAMAGE PROBABILITIES FOR TRIPLE IMPACT
3-6	TURBINE MISSILE HAZARD TO LTM TARGETS P_4 ANNUAL PROBABILITY OF DAMAGE

LIST OF FIGURES

- 2-1 GENERAL PLANT LAYOUT
- 2-2 PLANT LAYOUT ABOVE ELEVATIONS 568'-6", 574'-10", 577'-6" & 580'-6"
- 2-3 PLANT LAYOUT ABOVE ELEVATIONS 593'-6", 599'-0", 600'-6", 602'-6" & 605'-6"
- 2-4 PLANT LAYOUT ABOVE ELEVATIONS 620'-6", 623'-6" & 624'-6"
- 2-5 PLANT LAYOUT ABOVE ELEVATIONS 638'-6", 642'-0" & 647'-6"
- 2-6 PLANT LAYOUT SECTION A-A
- 2-7 PLANT LAYOUT SECTION B-B
- 2-8 MISSILE DIMENSIONING
- 3-1 MISSILE GENERATION ORIGINS
- 3-2 RESIDUAL PERFORATION VELOCITIES FOR WHEEL GROUP I THROUGH 6" STEEL BARRIER
- 3-3 RESIDUAL PERFORATION VELOCITIES FOR WHEEL GROUP II THROUGH 6" STEEL BARRIER
- 3-4 RESIDUAL PERFORATION VELOCITIES FOR WHEEL GROUP III THROUGH 6" STEEL BARRIER
- 3-5 RESIDUAL PERFORATION VELOCITIES FOR WHEEL GROUP I THROUGH 3' CONCRETE BARRIER
- 3-6 RESIDUAL PERFORATION VELOCITIES FOR WHEEL GROUP II THROUGH 3' CONCRETE BARRIER
- 3-7 RESIDUAL PERFORATION VELOCITIES FOR WHEEL GROUP III THROUGH 3' CONCRETE BARRIER
- 3-8 PROBABILITY HISTOGRAM FOR WHEEL GROUP III DESTRUCTIVE OVERSPEED MISSILES EXITING TURBINE BUILDING - 3' CONCRETE BARRIER
- 3-9 PROBABILITY HISTOGRAM FOR WHEEL GROUP III DESTRUCTIVE OVERSPEED MISSILES EXITING TURBINE BUILDING - 6" STEEL AND 3' CONCRETE BARRIER

INTRODUCTION

This document is submitted in support of the application of the Cleveland Electric Illuminating Company (CEI) to the Nuclear Regulatory Commission (NRC) for a construction permit for the Perry Nuclear Power Plant near Perry, Ohio. This report has been prepared using the guidelines set down by the NRC in Regulatory Guide 1.115, "Protection Against Low Trajectory Turbine Missiles", for the purpose of demonstrating the adequacy of the plant design with respect to turbine missile accidents.

This analysis is based on two wheel burst conditions:

- a. turbine failure at 120 percent of rated speed (design overspeed) and,
- b. failure at 180 percent of rated speed (destructive overspeed).

The turbine discs are designed for 120 percent overspeed condition, therefore, this failure would be caused by a flaw in the disc. The turbine discs are not designed for 180 percent of rated speed, therefore, this condition is postulated to result in ductile failure of the disc. The missiles produced by these failures may perforate the turbine casing with sufficient residual energy to cause damage to the remainder of the plant.

This analysis conservatively assesses the probability of a low-trajectory missile (LTM) damaging a safety-related structure or system which could potentially result in unacceptable consequences.

The probability of a missile being generated, subsequently striking any safety related structure or system and causing unacceptable consequences is demonstrated to be less than 1.5 E-8 per year per turbine as summarized in Table 3-6. Unacceptable consequences are defined in this case as damage which could prevent placing and/or maintaining the reactor in a safe shutdown condition. In determining these probabilities, the locations of vital equipment behind shield walls, building walls, and at elevations below the affected zones have been considered. These probabilities are well below those limits which would require design changes or modifications to the plant.

GENERAL DESCRIPTION

This section includes physical characteristics of both the Perry Nuclear Power Plant and the postulated turbine missile. Sections 2.1 and 2.2 detail general plant design and vital strike targets in the plant. Mechanisms of plant failure are described in 2.3.

Turbine missile characteristics as supplied by General Electric Company are contained in 2.4. Table 2-2 furnishes information concerning the protection afforded to safety related plant structures and systems.

2.1

DESCRIPTION OF THE PERRY NUCLEAR POWER PLANT

The Perry Nuclear Power Plant is a two-unit boiling water reactor complex with the main turbines in a tangential arrangement. Plant buildings for each unit, including the major systems and equipment located in each, are described briefly as follows: (1)

a. Reactor Building Complex

The Reactor Building Complex consists of the Interior Structure (including Drywell and Suppression Pool), Containment Vessel, and Shield Building. These structures house and protect the reactor and some safety class equipment. The structures are supported by a common foundation-mat at elevation 574'-0" and are structurally separate from each other above the mat. The relationship of the structures is shown in Figures 2-1 thru 2-7. In the event of a loss-of-coolant-accident (LOCA) these structures function together to contain the released materials and energy.

The Shield Building functions to:

1. Form a biological shield for radiation from the reactor.
2. Provide weather and exterior missile protection for the Containment Vessel.
3. Provide a relatively leak tight structure so that the annulus exhaust gas treatment system can be used to minimize the escape of radioactive particles to the environment, by maintaining the annulus air space at a slight negative pressure.

The Shield Building is a reinforced concrete structure consisting of a flat foundation mat, a cylindrical wall, and a shallow dome. General configuration of the Shield Building and its relation to other structures of the Reactor Building Complex is shown in Figure 2-6.

The Shield Building cylindrical wall extends from the top of the foundation mat to elevation 748.75 ft and is 136 ft O.D. with a wall thickness of 3 ft. The shallow dome has a radius of 120 ft with a wall thickness of 2.5 ft. The ring girder at the top of the cylindrical wall provides the only support for the dome.

The Containment Vessel is a pressure retaining structure composed of a steel cylinder and ellipsoidal dome secured to a steel lined reinforced concrete foundation mat. The mat is the common foundation for the three major structures of the Reactor Building Complex.

The Containment Vessel is designed to contain radioactive material which might be released from the nuclear steam supply system following a loss of coolant accident. The steel Containment Vessel ensures a high degree of leak tightness during normal operating and accident conditions.

Basic dimensions of the Containment Vessel are:

1. cylinder inside diameter 120 ft.
2. cylinder height 152.17 ft.
3. ellipsoidal dome ratio 2:1
4. cylinder thickness 1.5 in.
5. ellipsoidal dome thickness 1.25 in.

b. Turbine Building

The Turbine Building (including the Turbine Power Complex and Heater Bay) houses the power conversion system, including the turbine generator unit, main condenser, condensate pumps, air ejectors, turbine gland seal condensers, condensate demineralizers, the feedwater heating system, reactor feedpumps, and the circulating water system.

c. Control Complex

The Control Complex provides integrated control of the reactor, turbine generator, and auxiliary support systems, including reactor safety systems. This structure is common to both units.

d. Auxiliary Building

The Auxiliary Building houses the safety related systems consisting of sumps, heat exchangers, and piping which are used during and after plant shutdown or following a loss-of-coolant accident. These systems include the Residual Heat Removal (RHR), Low Pressure Coolant Injection (LPCI), High Pressure Core Spray (HPCS), and Reactor Core Isolation Cooling (RCIC) systems.

e. Fuel Handling Intermediate Building

The Fuel Handling Intermediate Building houses the fuel storage and handling facilities and some radwaste equipment. This building is common to both units.

f. Radwaste Building

The Radwaste Building houses various liquid and solid radwaste processing systems. This building is common to both units.

g. Offgas Building

The Offgas Building houses equipment used to treat gaseous radioactive effluents drawn from the main condenser by the air ejector.

h. Diesel Generator Building

The Diesel Generator Building houses the independent and redundant diesel generators that function as standby power sources in the event of loss of off-site power. This building is common to both units.

A summary of the safety classifications of the plant structures is given in Table 2-1. Relative locations of these structures is as shown in Figures 2-1 thru 2-7.

TABLE 2-1

SAFETY CLASSIFICATION AND LOCATION OF STRUCTURES

<u>Structure</u>		<u>Safety Class</u>	<u>Above Elev. 647.5 ft.</u>	<u>Below Elev. 647.5 ft.</u>
1.	Reactor Building Complex			
	Drywell	2	X	
	Containment Vessel	2	X	
	Shield Building	2	X	
2.	Auxiliary Building	2	X	
3.	Steam Tunnel between Auxiliary Building and Turbine Building	NSC*		X
4.	Fuel Handling Intermediate Building	2		X
5.	Radwaste Building	3		X
6.	Turbine Building	NSC*	X	
7.	Control Complex	3	X	
8.	Diesel Generator Building	3		X
9.	Off-gas Building	3		X
10.	Emergency Services Water Pump House	3		X
11.	Circulating & Service Water Pump House	NSC*		X
12.	Intake Structures & Cooling Water Tunnels	3		X
13.	Discharge Tunnel Entrance Structure and Downshaft	NSC*		X
14.	Discharge Tunnel and Diffuser Nozzle	3		X

* Non-Safety Class

NOTE: Turbine operating floor is at Elevation 647.5 ft.

Fig 2-1

General Plant Layout

11x17

E-036-020, Rev 9

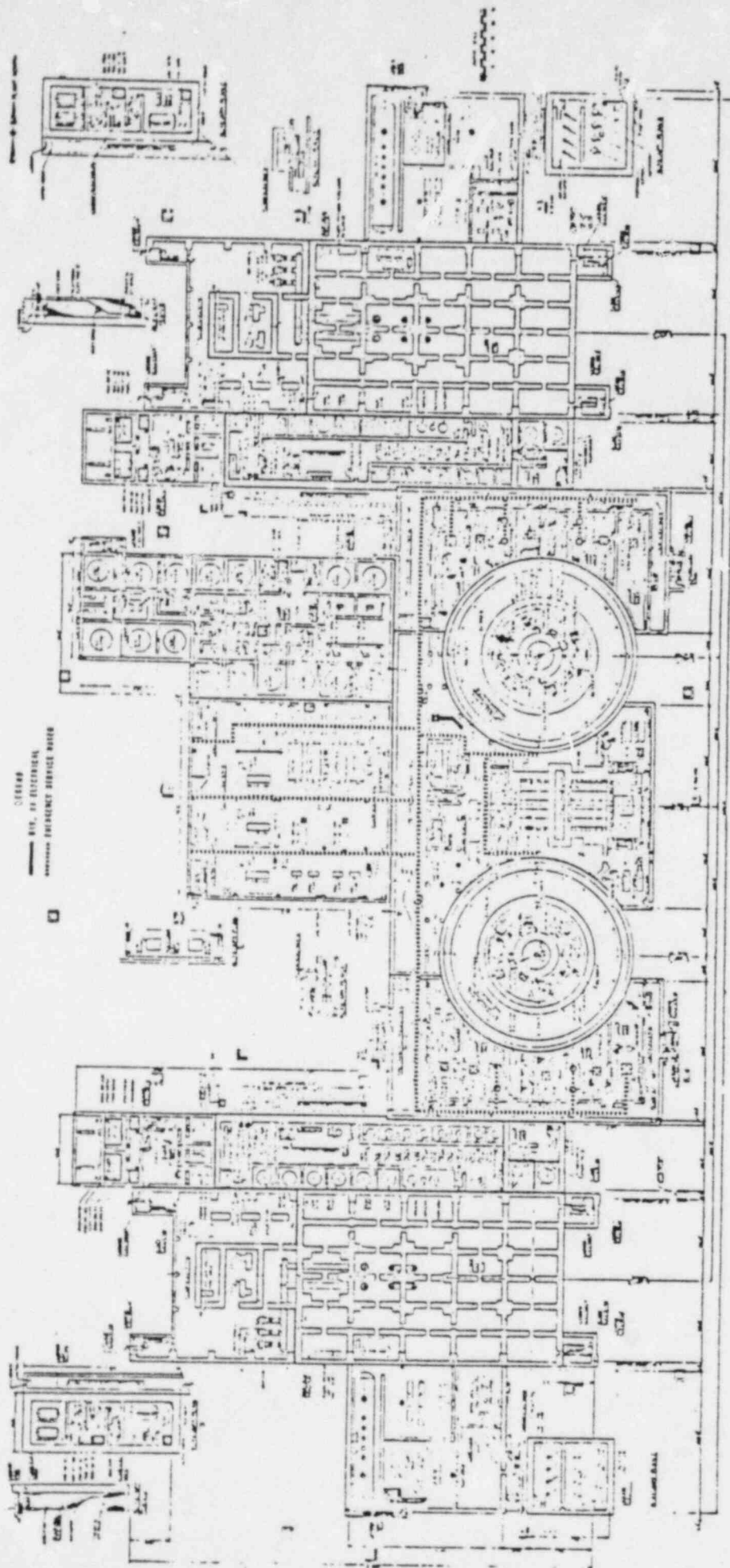


FIGURE 2-2
Title

(1411)

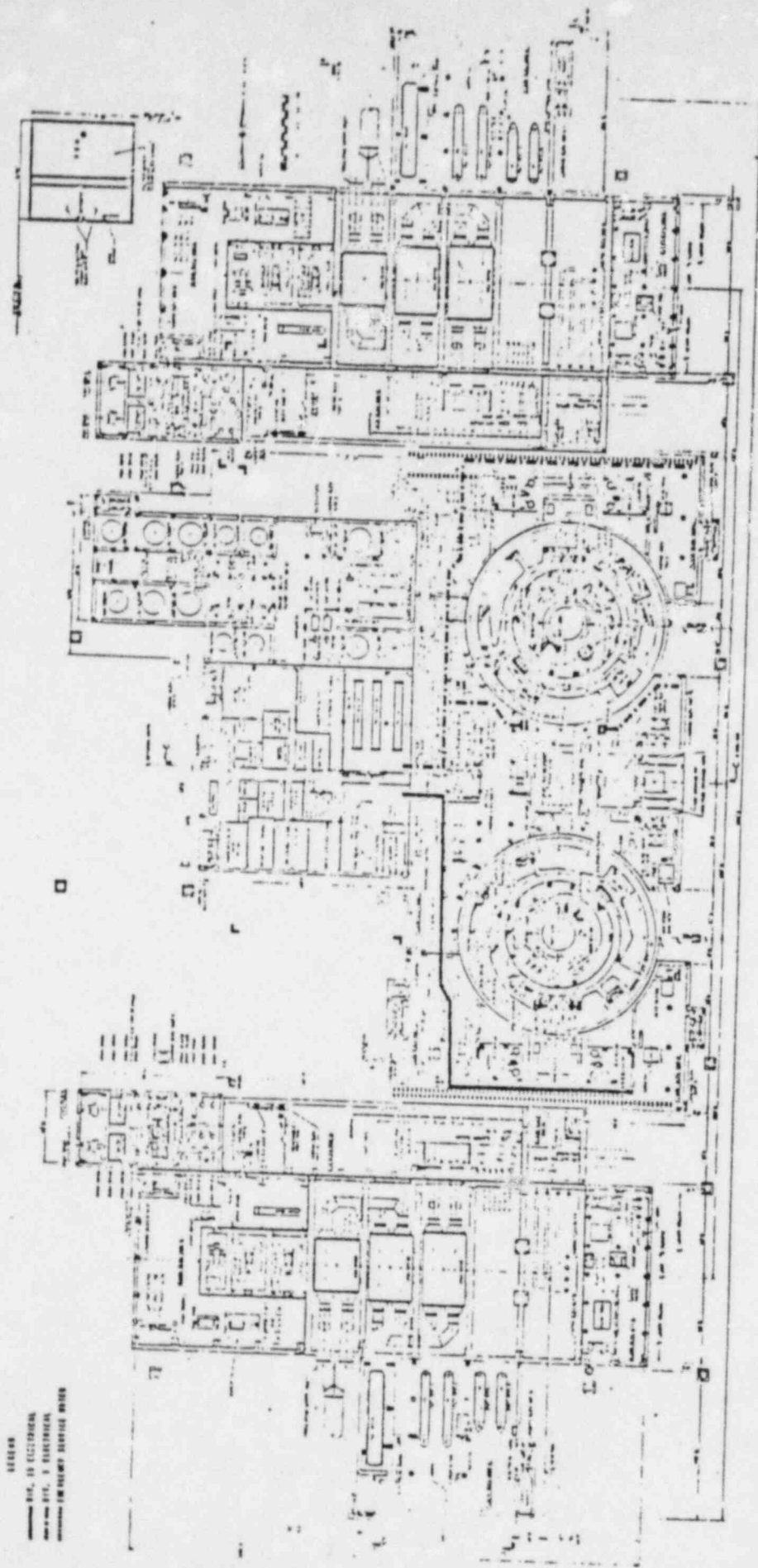


FIGURE 13
Teller

(11x17)

SECTION

— RAIL, IN EXISTENCE
— RAIL, IN EXISTENCE
— RAIL, IN EXISTENCE
— RAIL, IN EXISTENCE

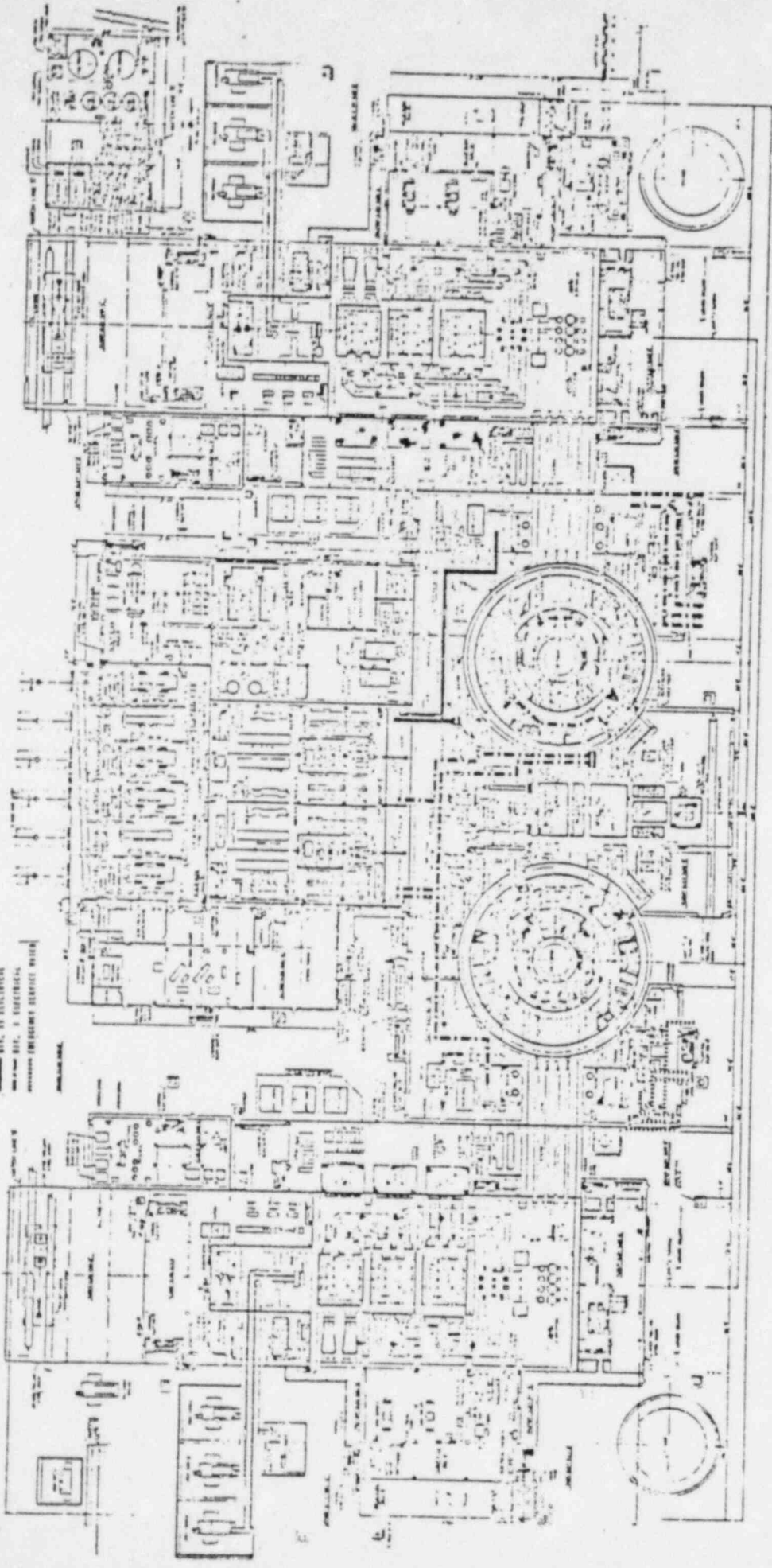


FIGURE 4

Title

1117

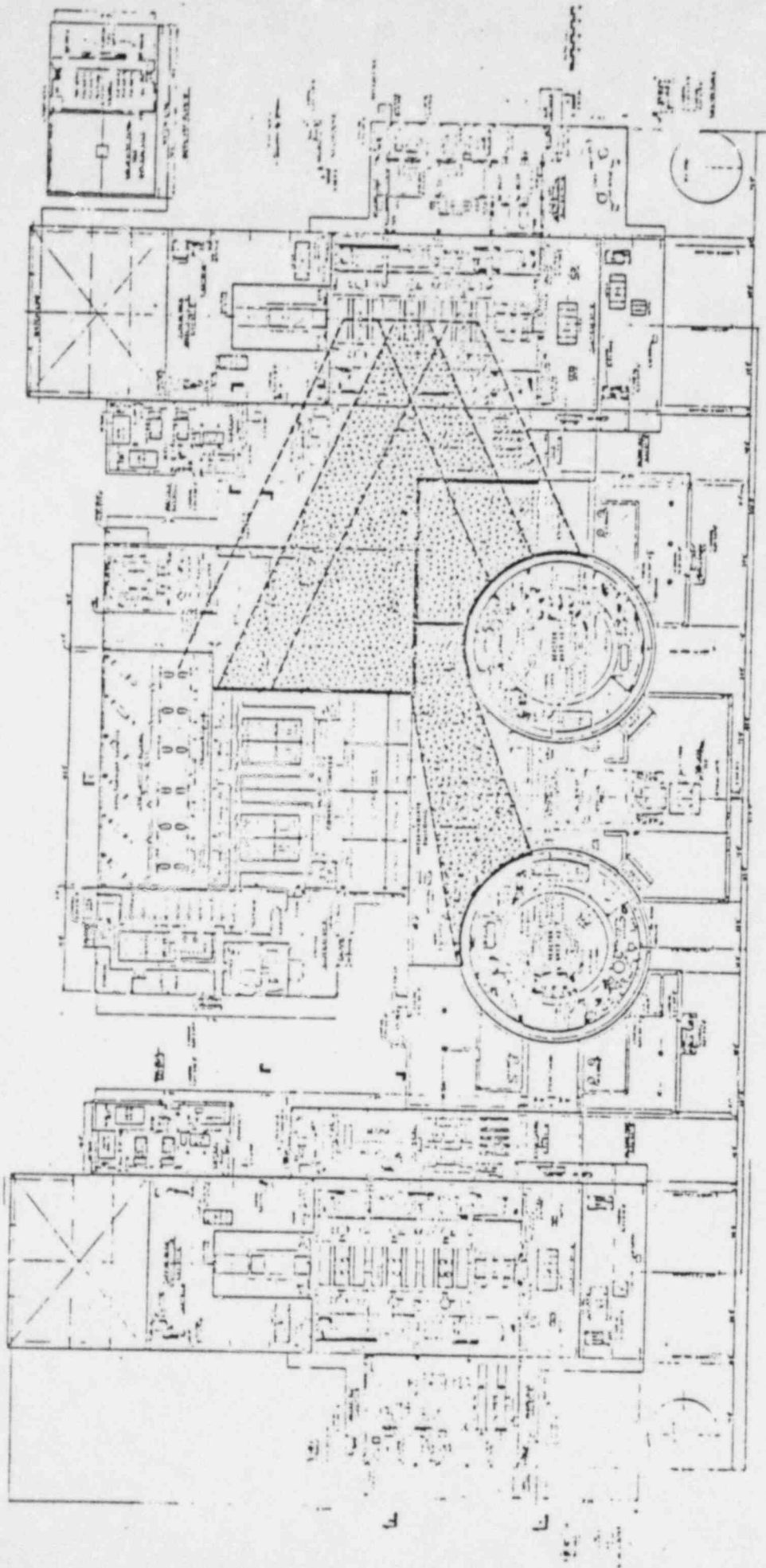
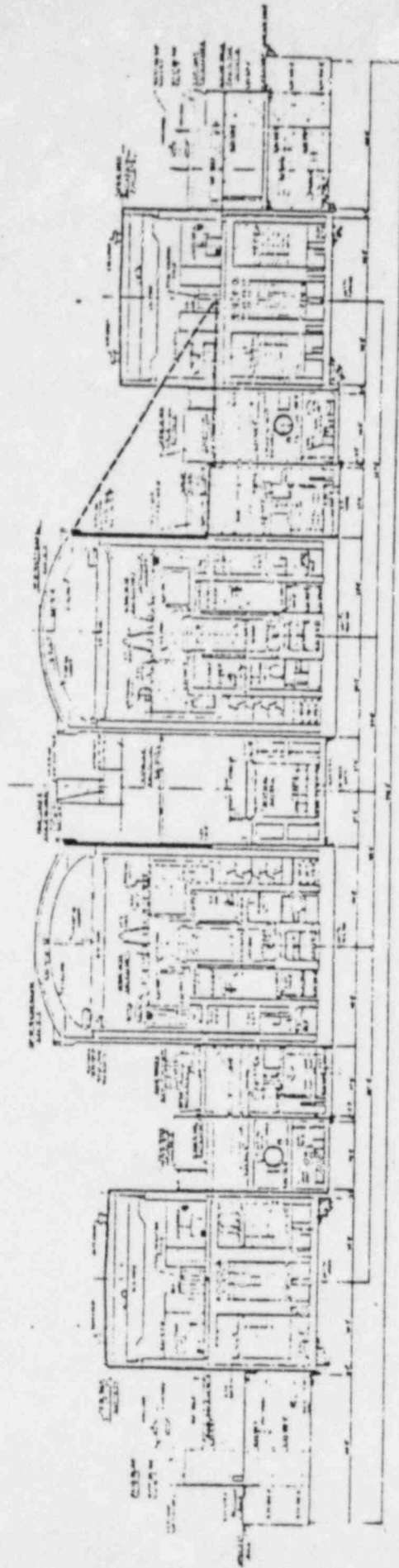


FIGURE 15
Title

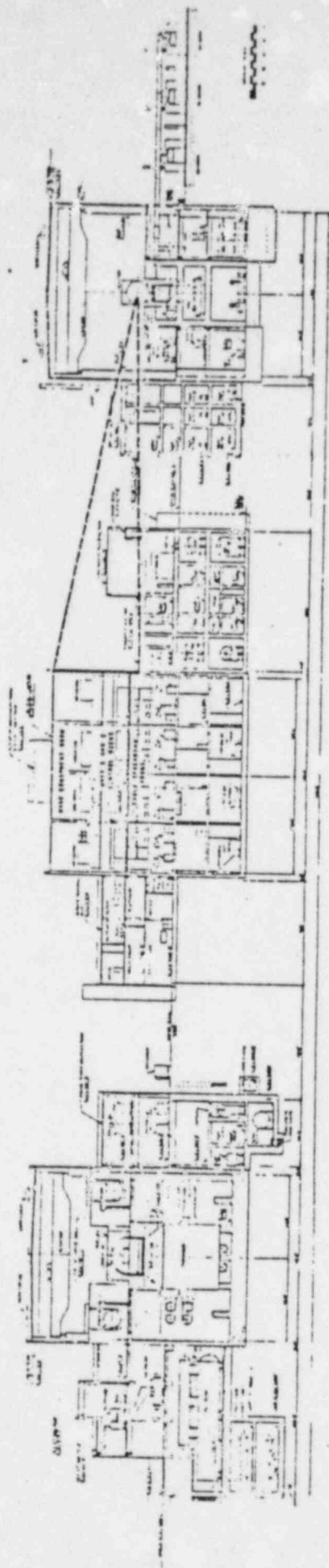
(11x17)



11x17

11x17

FIGURE 1-10
Title



11x17

FIGURE 17

Tilla

2.2

LOW TRAJECTORY MISSILE TARGET ZONE

The orientation of the Perry Unit 1 and 2 turbines establishes potential target areas on both units. These areas are depicted in Figures 2-1 thru 2-7 where missile ejection zones are defined by planes rotated 25° away from the wheel plane of the end stages of the low pressure turbines. The lower extremity of the LTM damage zone is defined as the turbine operating floor (elev. 647.5 ft). Safety related targets located either partially or completely within this zone include:

- a. Control Room
- b. Cable Spreading Room
- c. HVAC Equipment Room
- d. Intermediate Building
- e. Auxiliary Building
- f. Electrical Penetration Areas
- g. Unit 1 and 2 Reactor Building Complexes

Protective missile shielding barriers in the form of buildings, walls, and moisture separator (M/S) radiation shield are provided for all LTM targets. Table 2-2 summarizes the shielding barriers considered in this analysis. Allowable impact momenta appearing in Table 2-2 are discussed in Section 3.4.3. They appear here for future reference.

TABLE 2-2

PROTECTIVE BARRIERS FOR LTM STRIKE TARGETS

<u>Target</u>	<u>Barriers</u>	<u>Allowable Impact Momentum on Final Barriers (Kip - sec)</u>
Control Room Elev. 654.5 ft. to 679.5 ft.	2 ft. Control Bldg. Wall 3 ft. Turbine Bldg. Wall 6 in. M/S Radiation Shield	24
Cable Spreading Room Elev. 647.5 ft. to 654.5 ft.	2 ft. Control Bldg. Wall 3 ft. Turbine Bldg. Wall 6 in. M/S Radiation Shield	8.2
HVAC Equipment Room Elev. 679.5 ft. to 707.2 ft.	2 ft. Control Bldg. Wall 3 ft. Turbine Bldg. Wall 6 in. M/S Radiation Shield	24
Intermediate Bldg. Elev. 647.5 ft. to 707.5 ft.	4.5 ft. Intermediate Bldg. Wall 3 ft. Turbine Bldg. Wall 6 in. M/S Radiation Shield	56
Electrical Penetration Area Elev. 647.5 ft. to 654 ft.	4.5 ft. Intermediate Bldg. Wall 3 ft. Turbine Bldg. Wall 6 in. M/S Radiation Shield	56
Auxiliary Bldg. Elev. 647.5 ft. to 652 ft.	3 ft. Auxiliary Bldg. Wall 3 ft. Turbine Bldg. Wall 6 in. M/S Radiation Shield	17
Containment Vessel #1 Below Elev. 706 ft.	3 ft. Reactor Shield Bldg. Wall 3 ft. Turbine Bldg. Wall 6 in. M/S Radiation Shield	119
Containment Vessel #1 Above Elev. 706 ft.	3 ft. Reactor Shield Bldg. Wall 3 ft. Turbine Bldg. Wall	119

TABLE 2-2 (Cont'd)

<u>Target</u>	<u>Barriers</u>	<u>Allowable Impact Momentum on Final Barriers (Kip - sec)</u>
Containment Vessel #2 Elev. 647.5 ft. to 735 ft.	3 ft. Reactor Shield Bldg. Wall 2 ft. Intermediate Bldg. Roof 4.5 ft. Intermediate Bldg. Wall 3 ft. Turbine Bldg. Wall 6 in. M/S Radiation Shield	119
Containment Vessel #2 Above Elev. 735 ft.	3 ft. Reactor Shield Bldg. Wall 3 ft. Turbine Bldg. Wall 6 in. M/S Radiation Shield	119

Notes:

1. All building walls and roofs are 3000 psi concrete.
2. M/S radiation shield is 6 inch ASTM A-36 steel plate. M/S radiation shield is 144 ft. long and extends from Elev. 647.5 ft. to 663.25 ft. The radiation shield is hung from the Turbine Bldg. steel superstructure and is fastened together to act as one continuous plate.
3. The additional shielding effects of the moisture separator vessels have not been included in this analysis.
4. The Radwaste Building and Service Building have not been included as barriers due to their marginal shielding capabilities.

Determination of annual probabilities for events which could lead to unacceptable consequences due to turbine missile accidents is based upon a conservative set of plant damage assumptions.

Damage probabilities for non-redundant targets, e.g. Control Room, are based on the frequency with which such areas are penetrated or caused to lose structural integrity. No credit is taken for the potential of penetrating a target without causing a loss of safety function. Structures required to maintain structural and leak tight integrity, e.g. Containment Vessel, are similarly evaluated.

In the case of redundant shutdown components or systems, a concurrent single active failure in the redundant safety train is not considered, i.e., missiles generated from a turbine wheel burst must cause damage to both systems in order to lose shutdown capability.

Table 2-3 provides a summary of damage mechanisms used in this analysis by which unacceptable consequences are postulated.

TABLE 2-3

SUMMARY OF DAMAGE MECHANISMS FOR COMPROMISING UNIT SAFETY

<u>Direct Strike Target</u>	<u>Damage Mechanism</u>	<u>Events Leading to Potentially Unacceptable Consequences</u>
Control Room	Perforation, spallation or loss of structural integrity.	Unit 1 and/or 2 Control Rooms become non-operational.
Cable Spreading Room	Perforation, spallation, or loss of structural integrity.	Unit 1 and/or 2 Control Rooms become non-operational.
HVAC Equipment Room	Perforation or loss of structural integrity.	Possible collapse of HVAC equipment wall or ceilings onto Control Room below. Unit 1 or Unit 2 Control Rooms become non-operational.
Intermediate Bldg.	Perforation or loss of structural integrity.	Possible collapse of upper sections of Intermediate Bldg. onto Class 1-E cables and ESW piping.
Electrical Penetrations	Perforation or loss of structural integrity of exterior Intermediate Bldg. wall.	Damage to Div. 1 and Div. 2 electrical cables.
Auxiliary Bldg.	Perforation or loss of structural integrity.	Possible collapse of uppermost sections of Auxiliary Bldg. onto Class 1E electrical cables.
Containment Vessels	Perforation	Missiles perforating Reactor Shield Bldg. are assumed to perforate Containment Vessel.
	Loss of structural integrity.	Collapse of Reactor Shield Bldg. onto Containment Vessel and safety train electrical and piping penetrations.
	Spallation (not considered)	Containment Vessel is considered only as a spall barrier. Concrete debris in annulus can damage only Div. 1 safety train. Div. 2 penetrations are at the other side of the Reactor Shield Bldg.

TURBINE MISSILE CHARACTERISTICS

The two turbine-generator units for the Perry Nuclear Power Plant Units are manufactured by the General Electric Co. The steam turbines are tandem compound, six flow reheat, 1800 rpm units with 43 inch last stage buckets. Each turbine-generator unit has three low pressure turbines. There is a total of 42 low pressure turbine wheels.

The General Electric Co. provides data on turbine missiles originating in the low pressure units for use in evaluating plant damage hazards. ⁽²⁾ Reportedly, this data is based on an extensive experimental disc-bursting study performed by the turbine manufacturer. Because of similarities with regard to physical and geometric characteristics, this data is supplied in the form of three representative wheel groups. Individual wheel groups are further broken down into fragment groups ⁽²⁾. A summary of this data including weight, physical size, velocity, and energy ranges appears in Table 2-4 and Figure 2-8.

The total energies of the missile fragments have been calculated by Gonyea's method ⁽²⁾ in which missile ejection energy is defined as the difference between the kinetic energy of the wheel fragment at the instant of bursting and energy lost in penetrating stationary parts of the low pressure section. The energy values appearing in Table 2-4 are effective translational energies which include an additional component corresponding to the rotational energy of the missile fragment.

TABLE 2-4

43 INCH LAST STAGE BUCKET - LP TURBINE - MISSILE CHARACTERISTICS

Wheel Group I (stages 1-3)

Fragment group	a	b	c	d
Number of fragments in group	2	1	3	10
Sector angle, degrees	120	60		
Fragment weight, lbs.	2000	1000	300	100
Radius, in. R_1 , bore	20	20		
R_2 , hub	27	27		
R_3 , vane root	48	48		
Thickness, in. T_1 , hub	9	9		
T_2 , vane	3	3		
Approx. rectangular dimensions, in.			19x19x3	11x11x3
Design overspeed failure (120%)				
Minimum velocity, fps	0	0	0	0
Minimum energy, E+6 ft-lbs	0	0	0	0
Maximum velocity, fps	320	440	660	800
Maximum energy, E+6 ft-lbs	3	3	2	1
Destructive overspeed failure (180%)				
Minimum velocity, fps	0	0	0	0
Minimum energy, E+6 ft-lbs	0	0	0	0
Maximum velocity, fps	510	720	1000	1100
Maximum energy, E+6 ft-lbs	8	8	5	2

NOTES:

1. Data is representative of stage 2.
2. Sixteen missiles in four size classes are postulated to occur per burst.

TABLE 2-4 (Cont'd)

Wheel Group II (stages 4-6)

Fragment group	a	b	c	d
Number of fragments in group	2	1	3	10
Sector angle, degrees	120	60		
Fragment weight, lbs.	4000	2000	600	150
Radius, in. R_1 , bore	18	18		
R_2 , hub	27	27		
R_3 , vane root	47	47		
Thickness, in. T_1 , hub	12	12		
T_2 , vane	5	5		
Approx. rectangular dimensions, in.			20x20x5	10x10x5
Design overspeed failure (120%)				
Minimum velocity, fps	0	0	0	0
Minimum energy, E+6 ft-lbs	0	0	0	0
Maximum velocity, fps	340	440	660	660
Maximum energy, E+6 ft-lbs	7	6	4	1
Destructive overspeed failure (130%)				
Minimum velocity, fps	0	0	0	0
Minimum energy, E+6 ft-lbs	0	0	0	0
Maximum velocity, fps	520	720	930	930
Maximum energy, E+6 ft-lbs	17	16	8	2

NOTES:

1. Data is representative of stage 5.
2. Sixteen missiles in four size classes are postulated to occur per burst.

TABLE 2-4 (Cont'd)

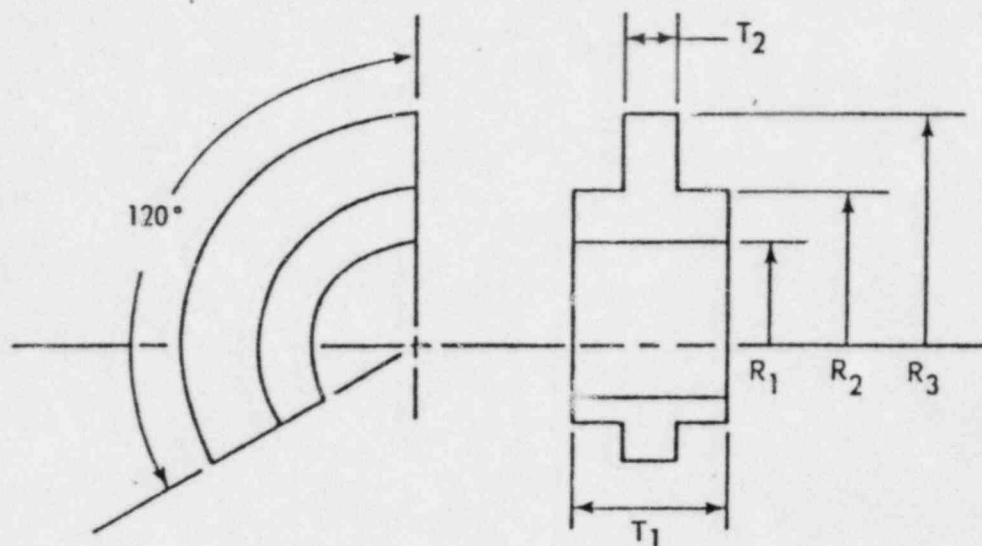
Wheel Group III (stage 7)

Fragment group	a	b	c	d
Number of fragments in group	2	1	3	10
Sector angle, degrees	120	60		
Fragment weight, lbs.	8200	4100	1400	200
Radius, in. R_1 , bore	17	17		
R_2 , hub	28	28		
R_3 , vane root	45	45		
Thickness, in. T_1 , hub	27	27		
T_2 , vane	12	12		
Approx. rectangular dimensions, in.			20x20x12	8x8x12
Design overspeed failure (120%)				
Minimum velocity, fps	280	0	0	0
Minimum energy, E+6 ft-lbs	10	0	0	0
Maximum velocity, fps	420	530	610	800
Maximum energy, E+6 ft-lbs	22	18	8	2
Destructive overspeed failure (180%)				
Minimum velocity, fps	450	0	0	0
Minimum energy, E+6 ft-lbs	26	0	0	0
Maximum velocity, fps	650	770	860	980
Maximum energy, E+6 ft-lbs	53	38	16	3

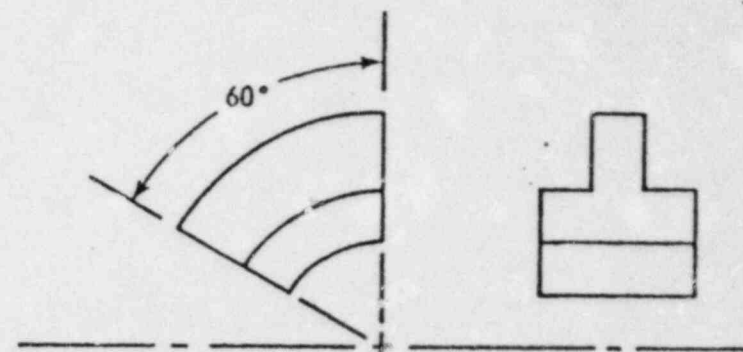
NOTES:

1. Data is representative of stage 7.
2. Sixteen missiles in four size classes are postulated to occur per burst.

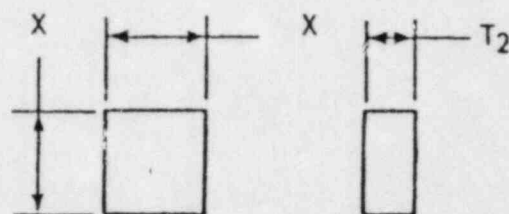
FRAGMENT GROUP a



FRAGMENT GROUP b



FRAGMENT GROUPS c AND d



3.0

EVALUATION OF TURBINE MISSILE DAMAGE PROBABILITY

This section details methods used to determine the risk due to low trajectory turbine missiles. Both deterministic and random sampling techniques are employed. For simplicity, only the risk associated with the Unit 1 turbine is addressed in this chapter. Based on symmetry arguments, the Unit 2 low pressure turbines have similar values.

3.1

INTRODUCTION

The P_4 damage probability for causing unacceptable damage to a safety related component or structure is comprised of the product of three contributing probabilities P_1 , P_2 , and P_3 . By definition:

P_1 = probability of turbine missile ejection

P_2 = probability that a missile is ejected in a spatial direction so as to impact a target

P_3 = probability of actually reaching a target and causing damage given the initial impact direction

Because these probabilities are often interrelated, each missile/target/trajectory combination can have its own unique P_4 value. Therefore, many individual P_4 values must be calculated and appropriately combined to yield the overall target risk.

A summary of the assumptions and methods used in determining P_4 and each of its constituent probabilities follows.

3.2 ANNUAL MISSILE EJECTION PROBABILITY - P_1

For this study, design (120 percent) and destructive (180 percent) overspeed turbine missile ejection probabilities of $9E-5$ and $4E-5$ events per year, respectively, have been used. These probabilities are based mainly on an analysis performed by Bush.⁽³⁾ Inclusion of the Gallatian turbine failure which occurred after Bush's work, has no appreciable effect on the design speed missile ejection probability.

As described in Section 3.1, each missile/target/trajectory combination must be examined. In determining the P_4 damage probabilities, it is convenient to define the P_1 for each missile origin-target combination as the annual probability of a given missile being generated at a given origin or location. Hypothetical missile generation origins are defined in Section 3.3. The individual annual ejection probability at each hypothetical missile generation origin is determined for each unit by multiplying the annual failure probabilities by the conditional probability of a given wheel failing at the particular location under consideration. All 42 low pressure turbine wheels are postulated to have equal failure probabilities. Therefore, the conditional probability of any particular disc failing is taken as 0.0238. The sum of all individual missile generation origin probabilities must equal the annual ejection probability for both the design and the destructive overspeed cases.

3.3 LTM STRIKE PROBABILITIES - P_2

3.3.1 Method

P_2 strike probabilities are calculated using simple solid angle arguments. Ejection of a missile fragment is assumed to be equally probable over the range of permissible solid angle ejection space. The probability of missile strike is then determined by integrating the differential solid angle $d\Omega$ over the limits defined by the available LTM impact area of the target. Therefore, P_2 is given by:

$$P_2 = \frac{\int_{\Omega \in A} f(\Omega) d\Omega}{\int_{\Omega \in A} d\Omega} = \frac{\int_{\Omega \in A} d\Omega}{2\pi(\sin \delta_u - \sin \delta_l)} \quad (1)$$

where δ_u , δ_l are the upper and lower wheel deflection angles.

For most LTM strikes Equation (1) can be adequately approximated in terms of the ground plane angle θ and elevation angle ϕ as

$$P_2 = \frac{\Delta\phi \Delta\theta}{2\pi(\sin \delta_u - \sin \delta_l)} \quad \delta_l \leq \theta \leq \delta_u \quad (2)$$

$$P_2 = 0.0 \quad \theta \notin \{\delta_l, \delta_u\}$$

where $\Delta\phi$ and $\Delta\theta$ are the maximum subtending elevation and range angular intervals respectively. A derivation of Equation 2 appears in Appendix B.

For inner wheel disc bursts, low pressure turbine discs 1 through 6, the range of δ is taken as $\pm 5^\circ$ from the plane of the wheel disc; for end stage wheel discs $\delta_l = 0^\circ$ and $\delta_u = 25^\circ$.⁽⁴⁾

3.3.2

LTM Strike Probabilities

All LTM strike probabilities have been conservatively evaluated using the minimum distance from the origin of missile generation to the particular target in question. The θ ground plane angular limits used correspond to the maximum angular range subtending the particular target region under consideration, except for the Shield Building where an effective concrete thickness of 7.5 feet has been used to determine the limits.

All missiles ejected in the direction of the turbine operating floor (Elev. 647.5 ft) are assumed to be contained within the concrete turbine pedestal complex and/or condenser areas. The turbine pedestal complex includes the turbine support girders which form a shield in excess of 10 feet of concrete on either side of, and parallel to, the turbine. A missile impacting either of these areas presents no safety hazard. Thus, all LTM zones have as a lower boundary the plane of the turbine operating floor. Table 3-1 presents the results of the P_2 strike probability calculations on Unit 1 and 2 from the assumed missile generation origins corresponding to the Unit 1 turbine.

All tabulated values are for a single missile. Nomenclature used in identifying the Unit 1 missile generation origins appears in Figure 3-1.

TABLE 3-1

LTM STRIKE PROBABILITIES

Target	Low Pressure Turbine A			Low Pressure Turbine B			Low Pressure Turbine C		
	E LSB*	Inner*	W LSB*	E LSB*	Inner*	W LSB*	E LSB*	Inner*	W LSB*
Control Room	0	3.1 E-3	1.4 E-2	6.1 E-4	1.1 E-2	1.5 E-2	1.3 E-2	1.5 E-2	1.1 E-2
Cable Spreading Room	0	8.3 E-4	3.9 E-3	1.8 E-4	3.1 E-3	4.4 E-3	3.7 E-3	4.4 E-3	3.2 E-3
HVAC Equipment Room	0	3.3 E-3	1.5 E-2	6.7 E-4	1.2 E-2	1.7 E-2	1.4 E-2	1.7 E-2	1.2 E-2
Intermediate Building	0	4.4 E-2	1.1 E-2	1.7 E-2	1.5 E-2	0	3.4 E-2	0	0
Electrical Penetrations	0	6.7 E-3	1.7 E-3	2.5 E-3	2.3 E-3	0	2.9 E-3	0	0
Auxiliary Building	5.4 E-3	6.4 E-3	2.8 E-3	6.4 E-3	9.6 E-4	0	3.8 E-3	0	0
Containment Vessel #1 Below Elev. 706 ft.	6.9 E-2	2.8 E-2	0	4.8 E-2	0	0	2.7 E-2	0	0
Containment Vessel #1 Above Elev. 706 ft.	2.9 E-2	1.1 E-2	0	2.0 E-2	0	0	1.0 E-2	0	0
Containment Vessel #2 Below Elev. 735 ft.	0	0	0	5.7 E-3	3.4 E-3	0	1.1 E-2	0	0
Containment Vessel #2 Above Elev. 735 ft.	0	0	0	9.8 E-4	3.3 E-4	0	2.2 E-3	0	0

* NOTE: E LSB = East Last Stage Bucket

W LSB = West Last Stage Bucket

Inner = Inner Stage Bucket

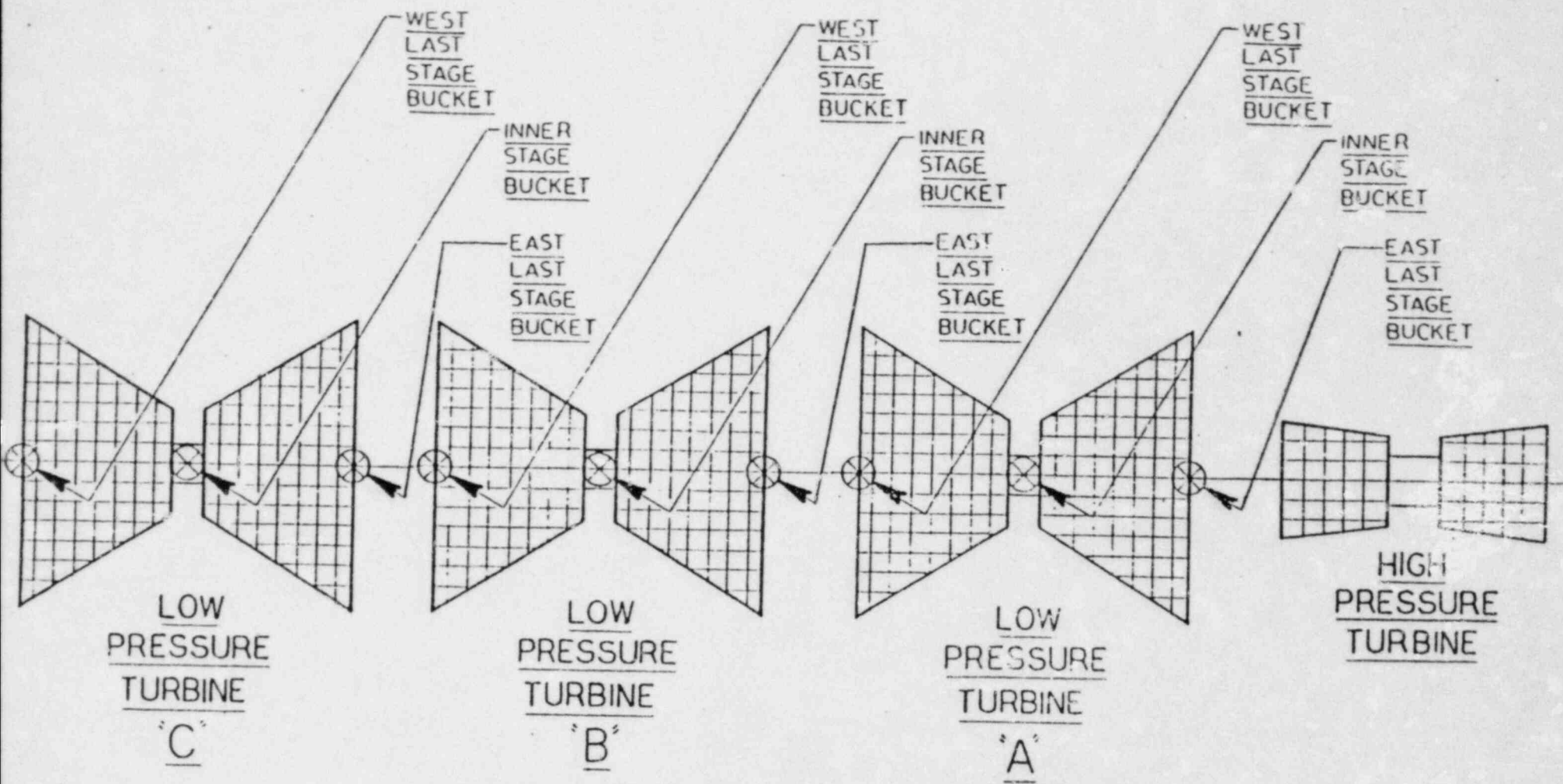


FIGURE 3-1

3.4 - DAMAGE PREDICTION - P_3

P_3 is defined in this analysis in terms of the probability of a missile actually reaching a target given the condition that it is ejected in the direction of the target. The effects of intervening barriers are included in the determination of P_3 . Note, that the target is considered irreconcilably damaged if the missile should breach the target boundary.

3.4.1 Method

The P_3 damage probability is evaluated by a Monte Carlo approach for representative LTM trajectories throughout the plant.

Initial missile ejection velocity and impact area are determined by random sampling techniques. Evaluation of barrier response to a particular missile is made by deterministic perforation and residual velocity models. The process continues to the next barrier where a new impact area is selected. The impact velocity is taken as the residual velocity calculated from the previous barrier interaction. The process is stopped when the missile either (1) fails to perforate an intermediate barrier, or (2) reaches the final barrier. The final barrier is then tested for penetration and for acceptable structural response. If the final barrier fails either test, the target is considered damaged. This entire procedure continues several thousand times with differing initial velocities and impact areas until a damage probability can be statistically predicted for each fragment.

The remainder of this section presents the models and assumptions used in evaluating the P_3 damage probabilities.

3.4.2 Intermediate Barrier Interaction

Criteria used in determining barrier adequacy in shielding safety related targets are based upon penetration, perforation, residual energy, and missile impact parameters.

3.4.2.1 Steel Barriers

For calculation of turbine missile perforation of the steel radiation shield next to the turbine, the Hagg-Sankey method detailed in Reference 5 is employed.

Containment of the missile by the steel barrier is a two stage process. Stage 1 involves inelastic impact and momentum transfer to an effective target mass. If perforation does not occur in Stage 1, the calculation proceeds to Stage 2 which includes the plastic strain capacity of the effective target mass. For perforation in Stage 1 or Stage 2, the residual energy and velocity are computed and used as input for the next barrier.

The effective mass of the target during Stage 1 is that portion of the steel shield that can respond to the missile during the initial contact and momentum transfer. The effective target mass is incorporated in the target resistance necessary for nonperforation in Stage 1 of the process. For nonperforation, the compressive strain energy, E_c , and shear strain energy, E_s , for the steel shield must exceed the energy that must be dissipated for momentum transfer, ΔE_1 , from the missile-target combination. Therefore, for nonperforation in Stage 1,

$$E_s + E_c > \Delta E_1 \quad (3)$$

If this inequality is not satisfied, perforation occurs and the residual velocity is calculated from energy and momentum considerations.

If the missile does not perforate the steel curtain in Stage 1, the process proceeds to Stage 2. In Stage 2, energy is dissipated by tension strain in the target. This tension strain energy, E_t , depends on the effective volume of target material strained and must be greater than the residual energy of the missile, ΔE_2 , after Stage 1 interactions for nonperforation. Therefore,

$$E_t > \Delta E_2 \quad (4)$$

for nonperforation, or containment, in Stage 2. Again, if this equality does not hold, perforation occurs and the residual velocity is calculated from energy considerations.

The effective mass of the target used in Stage 1 and Stage 2 calculations extends to plastic hinges 1.5 feet around the entire perimeter of the missile; this value corresponds to $3T$ as discussed in Reference 5, where T is the thickness of the target.

For calculation of the Stage 1 compressive strain energy, E_c , a relatively low value of strain equal to 0.07 is used. A strain value of 0.035 is used for the average tensile strain in Stage 2; this is the minimum value reported in Reference 5.

All impact geometrics are considered square. This assumption is conservative because it tends to minimize the effective target mass for any given impact area.

The dynamic strength factor used in the Hagg-Sankey formulation is calculated from the following fit of the data presented in Figure 17 of Reference 5:

$$\begin{aligned} \left[\frac{\sigma_d}{\sigma_u} \right] &= 8.89 - .674 \ln \sigma_u & \sigma_u \leq 78,000 \text{ psi} \\ \left[\frac{\sigma_d}{\sigma_u} \right] &= 1.30 & \sigma_u > 78,000 \text{ psi} \end{aligned} \tag{5}$$

where σ_d = dynamic strength of M/S steel radiation shield, psi.

σ_u = ultimate strength of M/S steel radiation shield, psi.

An ultimate strength of 69,700 psi is used for 6 inch thick ASTM A-36 plate. This is an average value obtained from vendor contacts.

Figures 3-2 thru 3-4 provide residual perforation velocities after perforation of a 6 inch A-36 steel plate as a function of impact velocity for various turbine missiles. Discontinuities in the curves indicate transition between Stage 1 and 2 phenomena. Minimum missile impact areas have been used in all cases (See Section 3.4.4).

A comparison of the residual velocities as predicted by the Hagg-Sankey method and an extension of the BRL steel perforation formula appears in Appendix A.

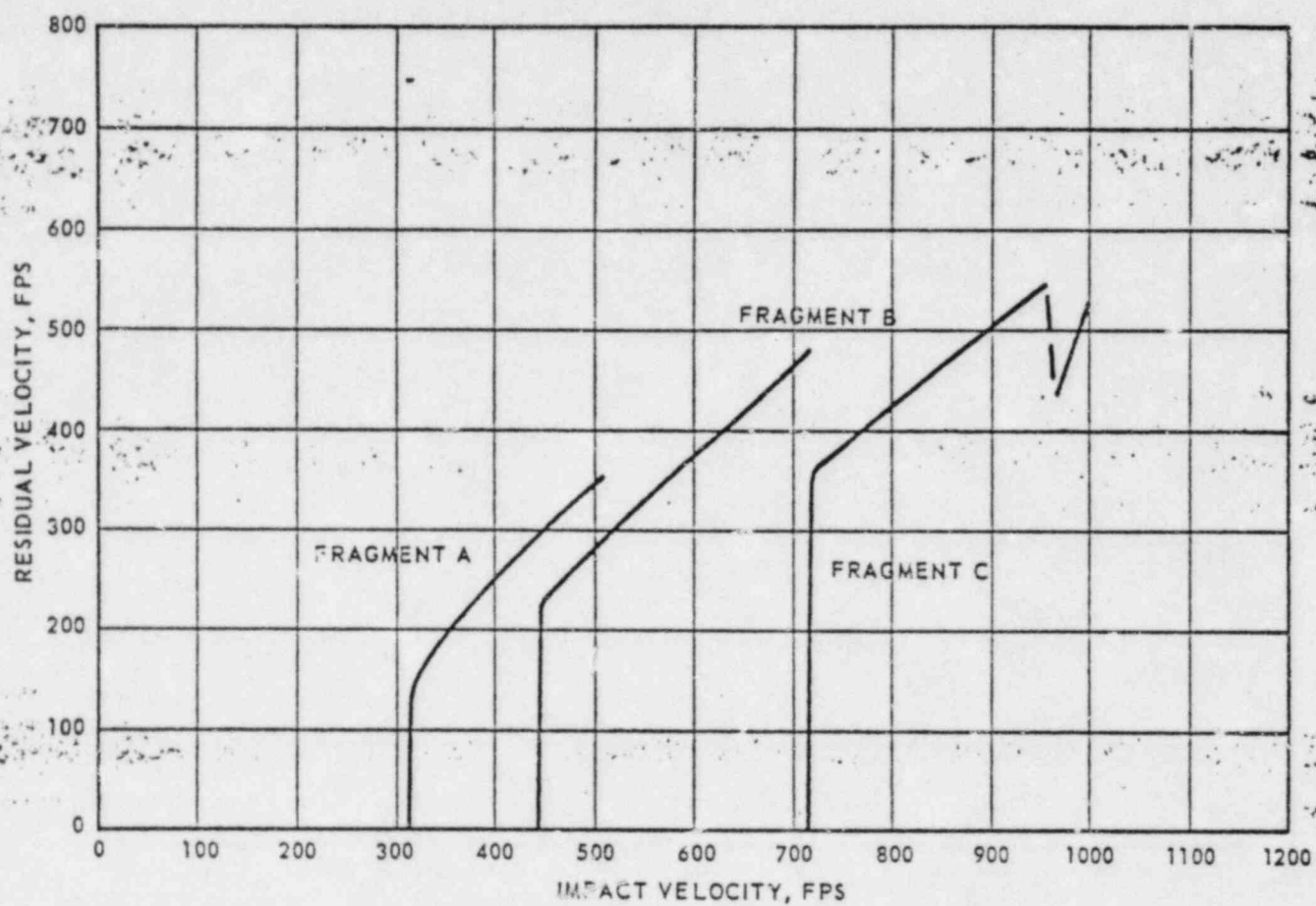


FIGURE 3-2
RESIDUAL PERFORATION VELOCITIES FOR
WHEEL GROUP I THROUGH 6" STEEL BARRIER

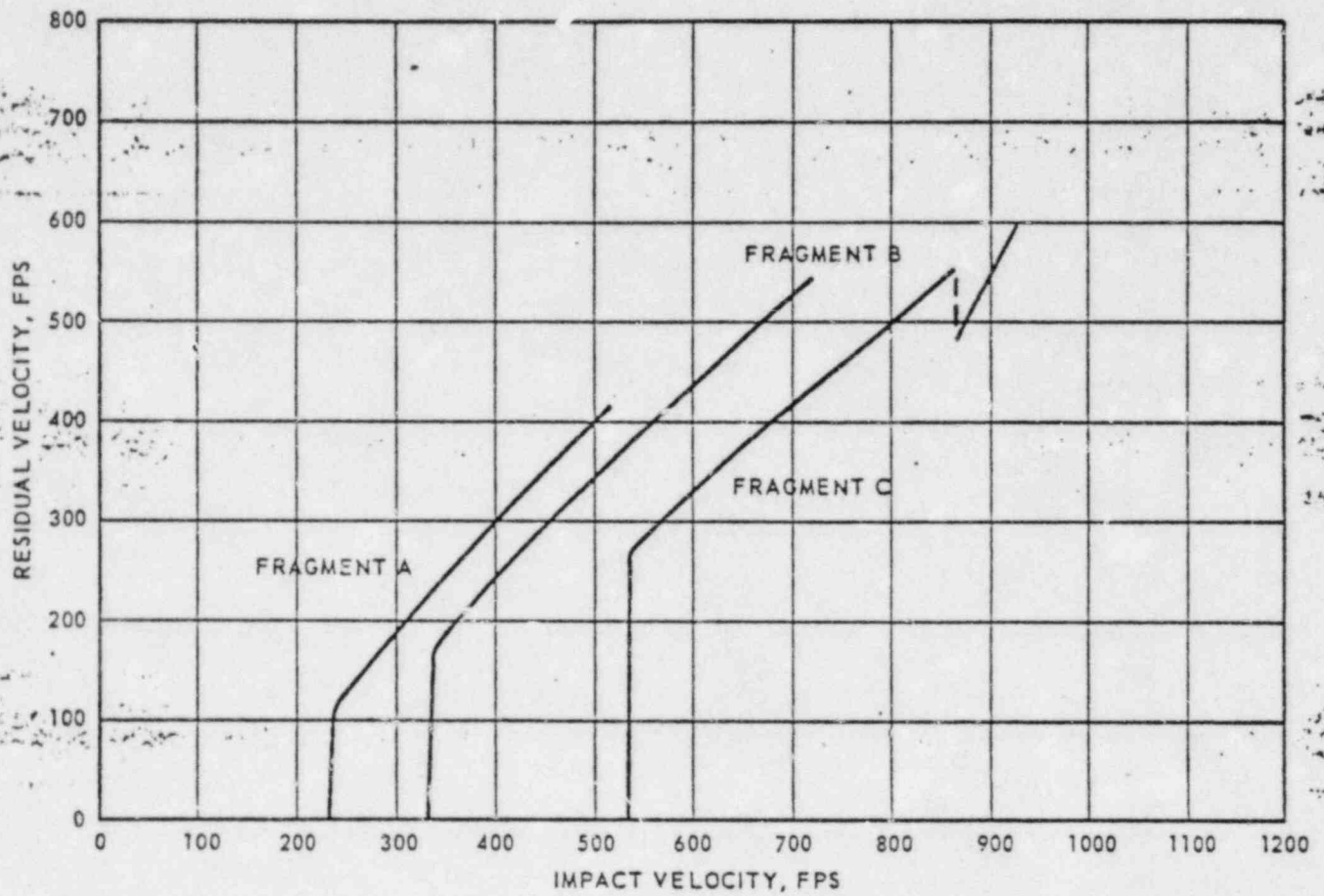


FIGURE 3-3
RESIDUAL PERFORATION VELOCITIES FOR
WHEEL GROUP II THROUGH 6" STEEL BARRIER

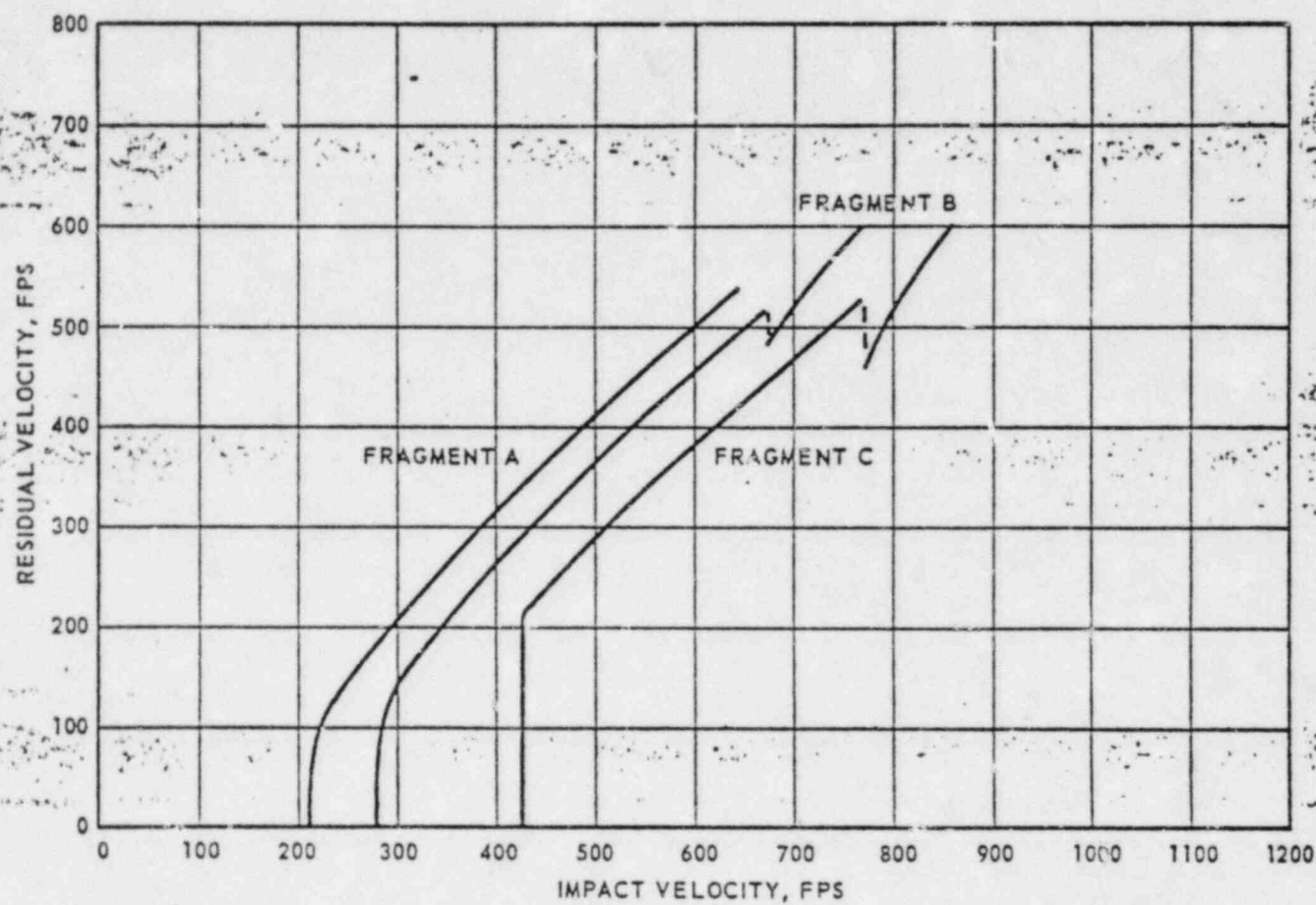


FIGURE 3-4
RESIDUAL PERFORATION VELOCITIES FOR
WHEEL GROUP III THROUGH 6" STEEL BARRIER

3.4.2.2 - Concrete Barriers

3.4.2.2.1 Penetration and Perforation

Missile penetration into an infinitely thick slab of concrete is predicted by the empirical Petry relationship.

$$D = K A_p \log_{10} \left[1 + \frac{v^2}{215,000} \right] \quad (6)$$

where,

D = the penetration depth, ft

K = an empirical penetration coefficient, ft³/lb

A_p = the sectional pressure of the missile, obtained by dividing the missile weight (W) by the appropriate missile frontal area (A), lb/ft².

V = the missile velocity, ft/sec.

For finite concrete thicknesses, the following modification is employed

$$D' = D \left[1 + e^{-4(T/D-2)} \right] \quad (7)$$

where,

D = infinite slab penetration depth, ft.

D' = penetration depth in a finite thickness slab, ft.

T = slab thickness, ft.

If 2D is greater than or equal to T in Equation (7), where T is the concrete thickness in feet, then perforation of the barrier by the missile is indicated.

Impacts are considered to be head-on, which results in the minimum available concrete thickness to resist penetration. (6) This assumption is conservative especially with regard to the curved Shield Building wall surface. A penetration coefficient value, K, of $0.0042 \text{ ft}^3\text{-lb}^{-1}$ has been assumed for 3000 psi concrete. This constant appears to be a reasonable value from available literature. (3) (6) (7)

3.4.2.2.2 Perforation Residual Velocities

For those barriers that are perforated, the residual velocity, v_r , is calculated from energy considerations.

The residual kinetic energy E_r of the missile after perforation is defined as the difference between the missile at impact E_i , and that energy required to just perforate the barrier E_p .

$$E_r = E_i - E_p \quad (8)$$

In Equation (8) no credit is taken for that portion of the impact energy that is dissipated in deformation or cracking and splintering of the target barrier; i.e. impact and perforation are considered local events.

The residual velocity, v_r , after perforation of a barrier is determined by substitution of Equation (6) and (7) into Equation (8) as

$$v_r = \sqrt{v_i^2 - 215,000 \left\{ 10^{T/(2KA_p)} - 1 \right\}} \quad (9)$$

where

v_i = the initial impact velocity corresponding to the impact energy E_i , (fps).

- All other variables in Equation (9) have been previously defined.

Figures (3-5) through (3-7) provide residual velocities after perforation of a three foot thick 3000 psi concrete slab as a function of impact velocities for various turbine missiles. Minimum impact areas have been used in all cases. (See Section 3.4.4)

A comparison of the residual velocities predicted by Equation (9) and that of the BRL concrete perforation formula appears in Appendix A.

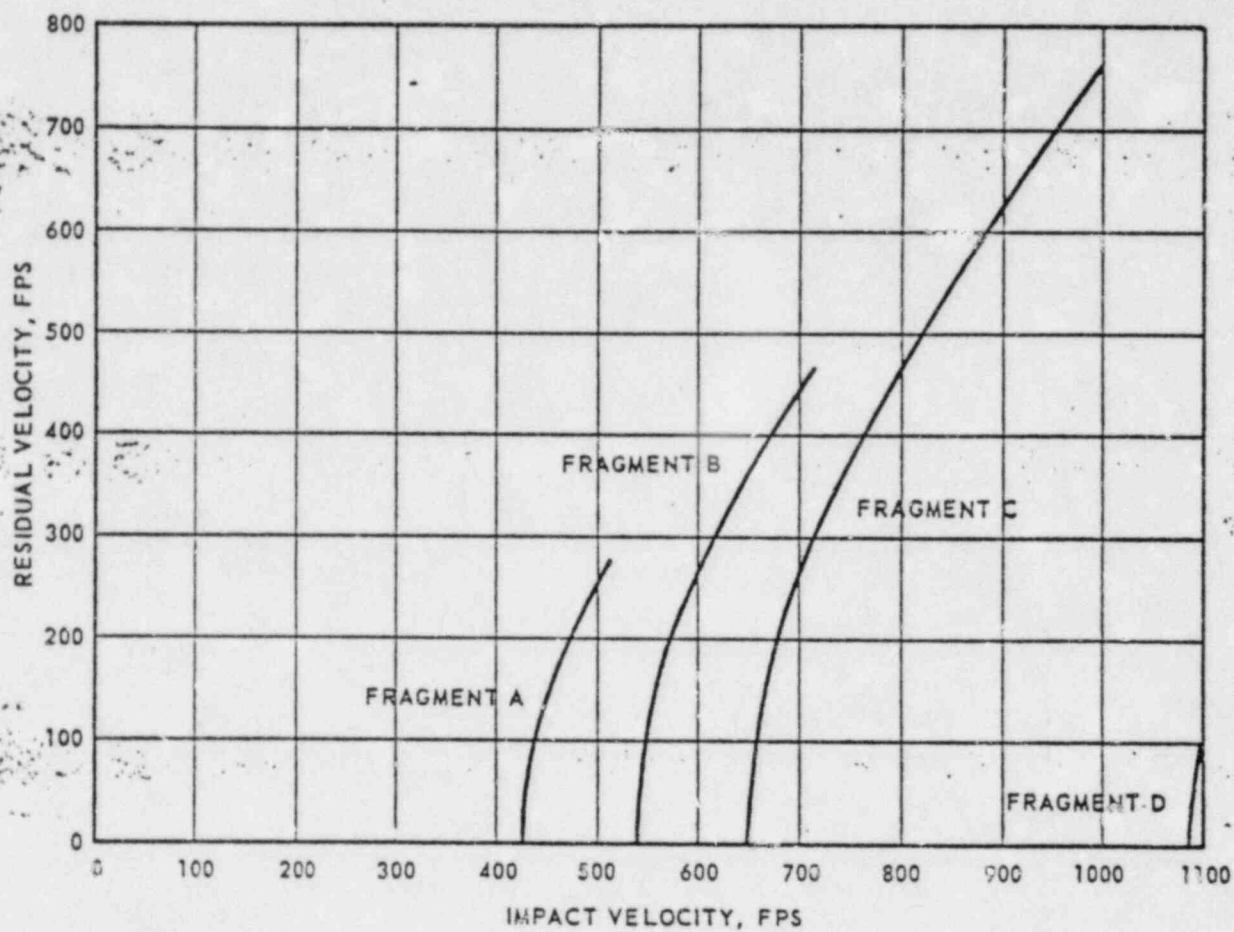


FIGURE 3-5
RESIDUAL PERFORATION VELOCITIES FOR
WHEEL GROUP I THROUGH 3' CONCRETE BARRIER

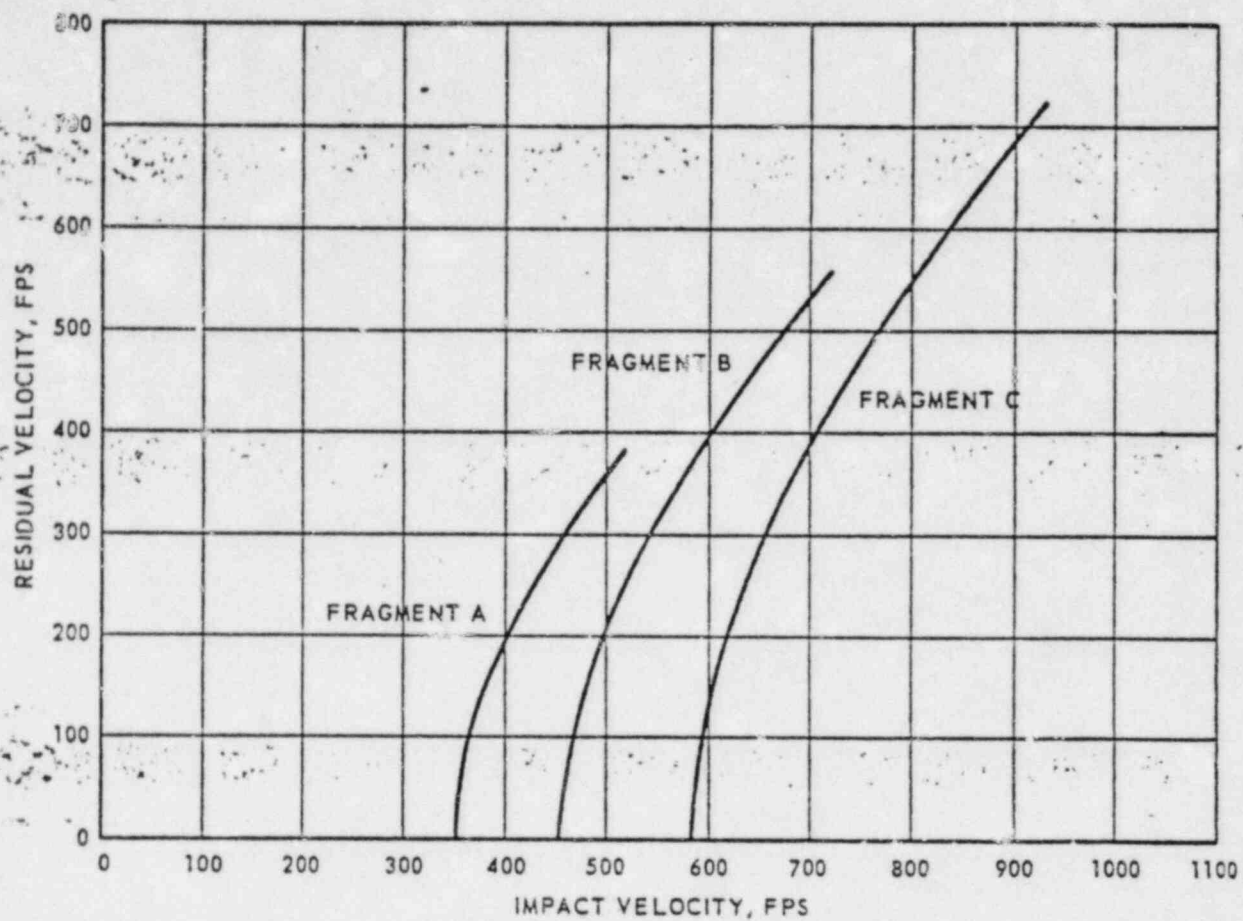


FIGURE 3-6
RESIDUAL PERFORATION VELOCITIES FOR
WHEEL GROUP II THROUGH 3' CONCRETE BARRIER

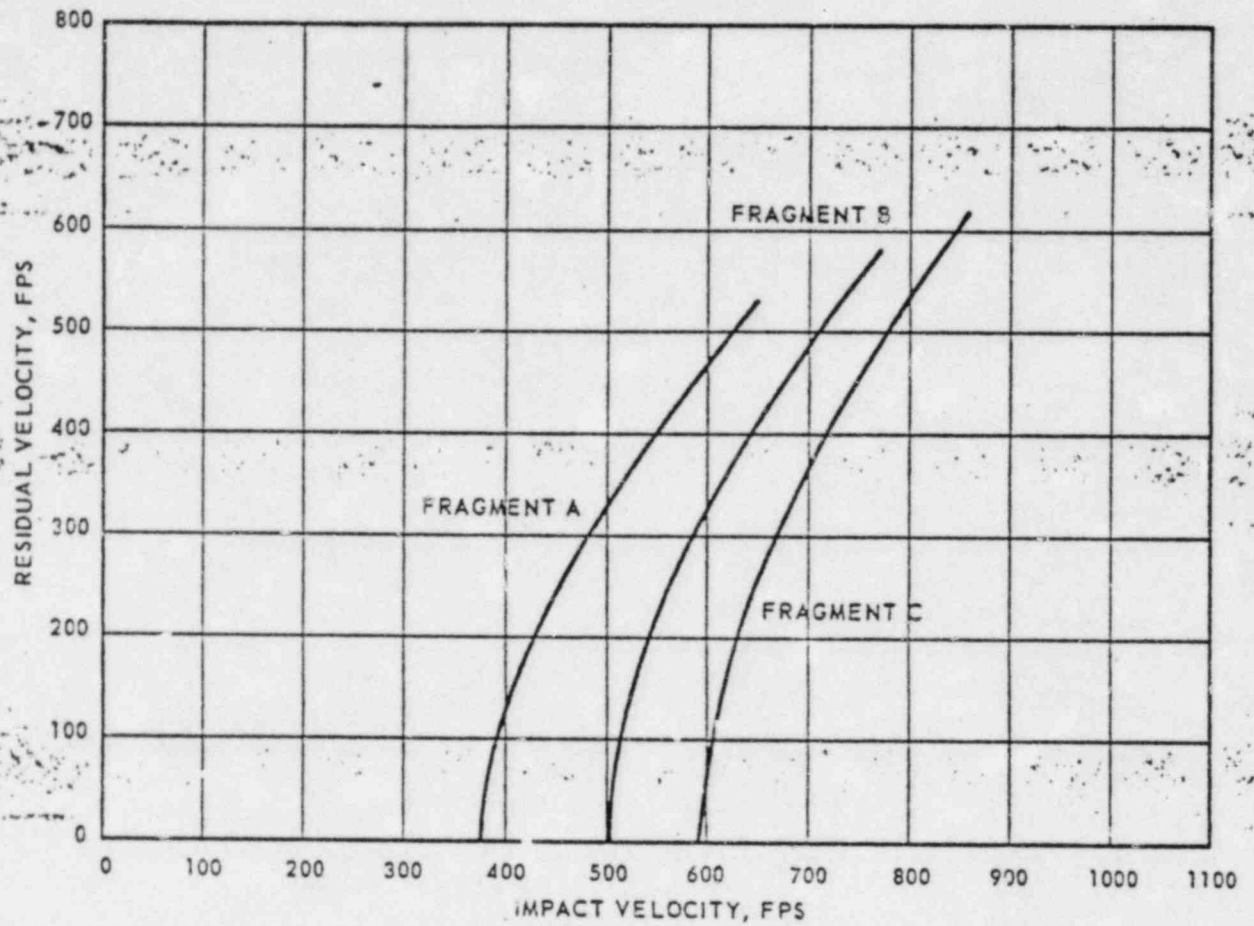


FIGURE 3-7
RESIDUAL PERFORATION VELOCITIES FOR
WHEEL GROUP III THROUGH 3' CONCRETE BARRIER

3.4.3 - Final Barriers

The adequacy of final barriers is evaluated by consideration of perforation, penetration, and overall structural integrity after impact. Allowances are made for concrete spalling where this phenomena may provide some element of risk to plant safety.

3.4.3.1 Penetration and Perforation

Final barriers are checked for perforation and penetration using the methods of Section 3.4.2.1. Additional conservatism is obtained by use of a safety factor of 1.3 with Equation (7) for penetration in final barriers.

3.4.3.2 Spallation

For those final barriers where a spalling allowance is made, spalling is assumed to occur if

$$T < D' + S \quad (10)$$

where

T = the final barrier slab thickness, ft.

D' = the penetration depth in a finite thickness slab as calculated from Equation (7), ft.

S = the spalling allowance, ft.

The spalling allowance thickness is taken as one-half the thickness of the final barrier.

3.4.3.3 Structural Integrity

The analytical procedure used to determine the structural integrity of the final barriers is the same approach as found in Reference 8. The maximum static concentrated load is first calculated for the final barrier. For a reinforced concrete slab or wall, yield line theory is used to calculate the maximum concentrated load to cause the ultimate resisting moment of the slab or wall. For a beam the maximum concentrated load is that load that causes the ultimate resisting moment of the beam with the appropriate end conditions. Using these concentrated loads as the equivalent static loads, the momentum capacities of the final barriers are obtained. A ductility factor of 10.0 for reinforced concrete was used. Allowable impact momenta used for structural integrity evaluation appear in Table 2-2.

3.4.4 Missile Impact Parameters

In evaluation of the turbine missile threat to the plant, two parameters are randomly sampled. These parameters are turbine missile impact area and initial ejection velocity.

3.4.4.1 Missile Impact Area

Impact area definition for the type A and B fragment wheel sector missiles is treated conservatively by assuming that all missile barrier interactions occur with the missile on edge, i.e., any deflection of the missile onto its flat side is neglected.

The dynamic restraints on the smaller postulated missiles are considerably less than the turbine disc sector missiles. Therefore, the range of impact areas for type C and D rectangular missiles

- includes the likelihood that the missile will not strike the target on a flat end side. Credit is taken for oblique frontal impact by defining the upper limit of the area range for each fragment by⁽⁹⁾

$$A_{\max} = X^2 \sqrt{1 + 2 \frac{T^2}{X^2}} \quad (11)$$

where T and X are postulated missile thickness and square side dimensions respectively.

Reference (9) demonstrates for a 90° disc sector missile that a linear cumulative distribution approximation overestimates the actual impact area distribution. These results can be readily extrapolated to the 60° and 120° sector missiles used in this analysis. This same assumption is used in defining the distribution function for the C and D fragment groups. Table 3-2 provides the lower and upper impact areas limits used for each fragment.

3.4.4.2 Missile Ejection Velocity

Reference 2 presents no information on the missile ejection velocity distribution spectrum. In this analysis a uniform velocity distribution has been assumed for each fragment. The upper and lower bounds of the distribution correspond to the minimum and maximum casing exit velocities appearing in Table 2-4.

The assumption of a uniformly distributed velocity spectrum reflects the uncertainty in the velocity data from previous turbine failures and in the potential interactions occurring inside the turbine between wheel disc break up and casing perforation.

. From a statistical viewpoint, the actual distribution (if one could be measured or calculated) is most likely peaked and falls to zero as the end points are approached. The uniformity assumption is unrealistic at the maximum velocity in the sense that the distribution immediately drops to zero. It is conservative in that more higher velocity missiles are sampled and examined for potential damage.

TABLE 3-2

LOWER AND UPPER IMPACT AREAS

<u>Stage Group</u>	<u>Bound</u>	A	<u>Fragment Type</u>		D
			B	C	
I	Minimum	216	150	57	33
	Maximum	530	306	370	130
II	Minimum	316	235	100	50
	Maximum	734	423	424	122
III	Minimum	731	563	240	64
	Maximum	1662	960	525	150

NOTE:

1. All areas in inches².
2. All areas are minimum and maximum projected fragment areas calculated from data in Section 2.0.

3.4.5 Multiple Impacts

Six fragments are considered in the multistrike analysis. The six missiles are two "A" fragments, one "B" fragment, and three "C" fragments. The ten "D" fragments are small missiles corresponding to secondary missiles from casing perforation, turbine blading, disc rings, etc. These small missiles most likely would have a larger spatial emission distribution than the disc segments. Furthermore, their kinetic energies and penetrability throughout the plant are minimal compared to the other fragments. Therefore, all D group missiles are considered to be of minimal threat to the plant and are excluded from the multiple strike analysis.

3.4.5.1 Multiple Impact Configuration

An upper limit on the number of missile hits can be estimated by assuming that any individual missile can cause unacceptable damage to the plant, i.e. P_3 is assumed unity. All missiles are assumed to be generated with equal independent probability in all directions. Therefore, using a typical direct strike P_2 of 0.02 the upper estimate of damage due to multiple hits is estimated using the binominal distribution as

$$P(n \geq 4) = 1 - \sum_{n=0}^3 B(n, 6, .02) = 2.32 \text{ E-6} \quad (12)$$

$$P(n=3) = B(3, 6, .02) = 1.51 \text{ E-4}$$

The above values are conditional on an annual turbine failure probability of 10^{-4} yr^{-1} . Thus, up to three missile hits on a target should be considered in achieving a 10^{-7} yr^{-1} goal.

3.4.5.2 - Multiple Impact Method

There is currently no existing methodology for accurately predicting damage effects caused by multiple missile impact. However, it is possible to postulate a conservative criterion based on shield barrier adequacy to determine multiple impact damage probabilities. Missiles are examined for ability to perforate intermediate barriers in serial order for each impact configuration set. If a missile is stopped by a barrier the next missile in the configuration is started out at that barrier. No credit is taken for a barrier once it has been perforated. This process continues until the target is either damaged or the allotted number of missiles in the impact set has been expended.

Each multiple hit sequence is evaluated by the same Monte Carlo techniques used for single missile hits. Analysis of intermediate and final barriers are by the methods discussed in Section 3.4.2.

3.4.6 Statistics

3.4.6.1 Sample Mean

After processing N histories, the best estimate of the P_3 damage probability is the mean of the individual values X_n ($n = 1, N$) where for the n'th history:

$X_n = 1$ for a damaging missile strike

$X_n = 0$ for a nondamaging missile strike

Thus, the Monte Carlo estimate of the unknown, P_3 , is \bar{X} where

$$\bar{X} = \frac{1}{N} \sum_{n=1}^N X_n \quad (13)$$

3.4.6.2 Statistical Confidence

To place some statistical confidence on the P_3 value of Equation (13), the Shapiro-Wilk⁽¹¹⁾ test is used.

The N histories are grouped into G groups with M histories in each group such that $MG = N$. The sample mean of the g'th group is \bar{X}_g ,

$$\bar{X}_g = \frac{1}{M} \sum_{m=1}^M X_{m,g} \quad (14)$$

The overall sample mean for the N histories is then

$$\bar{X} = \frac{1}{G} \sum_{g=1}^G \bar{X}_g \quad (15)$$

which is identical to Equation (13).

The standard deviation of the G group averages about the average is

$$S_g = \sqrt{\frac{1}{G} \sum_{g=1}^G (\bar{X}_g - \bar{X})^2} \quad (16)$$

The distribution of the \bar{X}_g 's is by the Central Limit Theorem asymptotically normal for large M. Thus, even though the X_n 's are not normally distributed about \bar{X} , the \bar{X}_g 's are expected to be normally distributed about \bar{X} provided the number of histories M in each group is large enough.

For Monte Carlo results Burrows and MacMillan⁽¹¹⁾ suggest fixing the number of groups at $G = 25$. The Shapiro-Wilk test for a sample size of 25 is then evaluated in the following manner.⁽¹¹⁾

The \bar{X}_g 's are arranged in ascending order and relabeled y_i ($i = 1, 25$) where y_1 and y_{25} are the smallest and largest values, respectively. The value of the Shapiro-Wilk test, W, is computed from

$$W = \frac{\left[\sum_{i=1}^{25} a_i y_i \right]^2}{\sum_{i=1}^{25} y_i^2 - \frac{1}{25} \left[\sum_{i=1}^{25} y_i \right]^2} \quad (17)$$

where the $a_i = -a_{26-i}$ are given below⁽¹¹⁾

<u>i</u>	<u>a_i</u>
1	-0.4450
2	-0.3069
3	-0.2543
4	-0.2148
5	-0.1822
6	-0.1539
7	-0.1283
8	-0.1046
9	-0.0823
10	-0.0610
11	-0.0403
12	-0.0200
13	0.0000

The magnitude of W tests the departure from normality in the distribution of the \overline{X}_g 's. W will be less than 0.931 only 10 percent of the times that this test is applied to samples actually drawn from a normal distribution. Thus, if W is less than 0.931, the validity of the calculated standard deviation s_g is doubtful.

W will be less than 0.888 only 1 percent of the time that this test is applied to samples actually drawn from a normal distribution. If W is less than 0.888, the reliability of \overline{X} as an estimate of X is doubtful.

In evaluation of the various P_3 's the number of Monte Carlo histories N is chosen such that $W > 0.931$ except where noted.

3.4.7 Damage Probabilities

P_3 damage probabilities using the methods described in Section 3.4.1 to 3.4.6 are presented in this section. Zero P_3 damage probabilities appearing in the tables of this section correspond to no damaging hits for the number of Monte Carlo histories specified.

3.4.7.1 Single Missile Impacts

Single impact damage probabilities appear in Table 3-3 for the destructive overspeed case. Standard deviations appear in parenthesis. No D fragment missile has sufficient energy to perforate the M/S steel radiation shield. Probability histograms as a function of exit energy of the missiles in Wheel Group III escaping the Turbine Building are displayed in Figures 3-8 and 3-9.

Design speed missiles cannot perforate the M/S shield - three foot Turbine Building wall barrier combination. It is possible to just perforate the three foot Turbine Building wall if the design speed missile is ejected such that it clears the M/S radiation shield. However, it is not possible to damage the plant because of its small residual velocity. Therefore, all P_3 values for the design speed case are zero.

3.4.7.2 Multiple Impacts

Double impact P_3 damage probabilities appear in Table 3-4 for the destructive overspeed case. Design speed case double impact probabilities have been determined to be negligible and, therefore, are not included here.*

Each probability for a given combination type appearing in Table 3-4 includes random ordering of the constituent missiles. Thus, the P_3 probability for the set A-B includes the two subsets corresponding to (1) an A missile followed by a B missile, and (2) a B missile followed by an A missile. A total of 5,000 Monte Carlo histories is used in determining each subset probability.

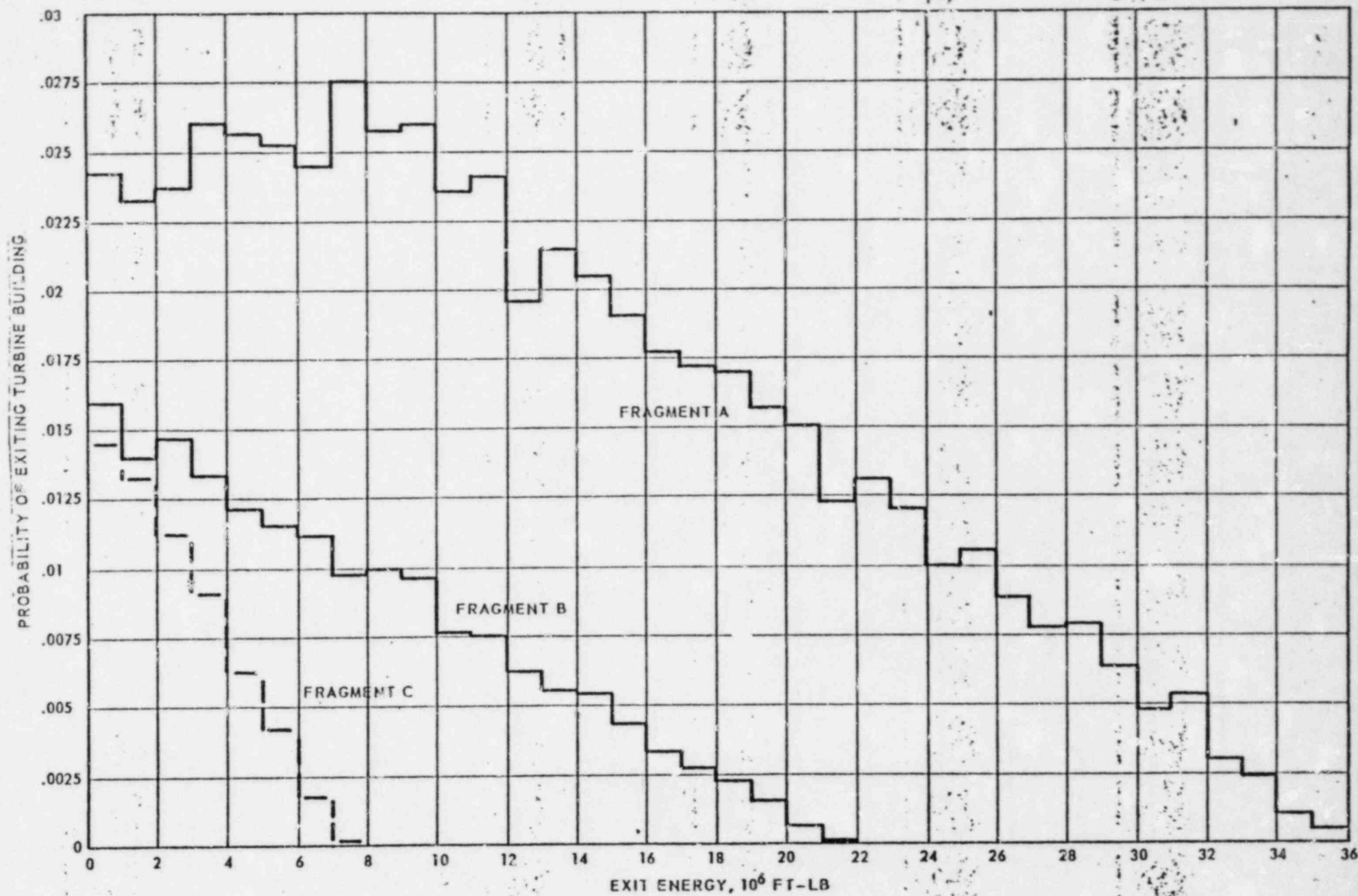
Triple impact damage probabilities have been evaluated for the Control Room and Containment Vessel at design and destructive overspeed. These probabilities are provided in Table 3-5. The procedural breakdown of each combination type into subsets is similar to the double impact case.

* For double impact configurations, the hazard to the plant from design speed missiles is two orders of magnitude lower than from destructive overspeed missiles.

A majority of the Wheel Group I and II multiple impact damage probabilities fail the Shapiro-Wilk test of Section 3.4.6.

The poor statistics are the result of calculating the probability of infrequently occurring events with moderate amounts of Monte Carlo histories, i.e., 10,000 to 15,000 histories per impact configuration. These small probability values are point estimates of the expected damage event. They have no significant effect on the results of the study.

FIGURE 3-8
PROBABILITY HISTOGRAM FOR WHEEL GROUP III DESTRUCTIVE
OVERSPEED MISSILES EXITING TURBINE BUILDING -
3' CONCRETE BARRIER



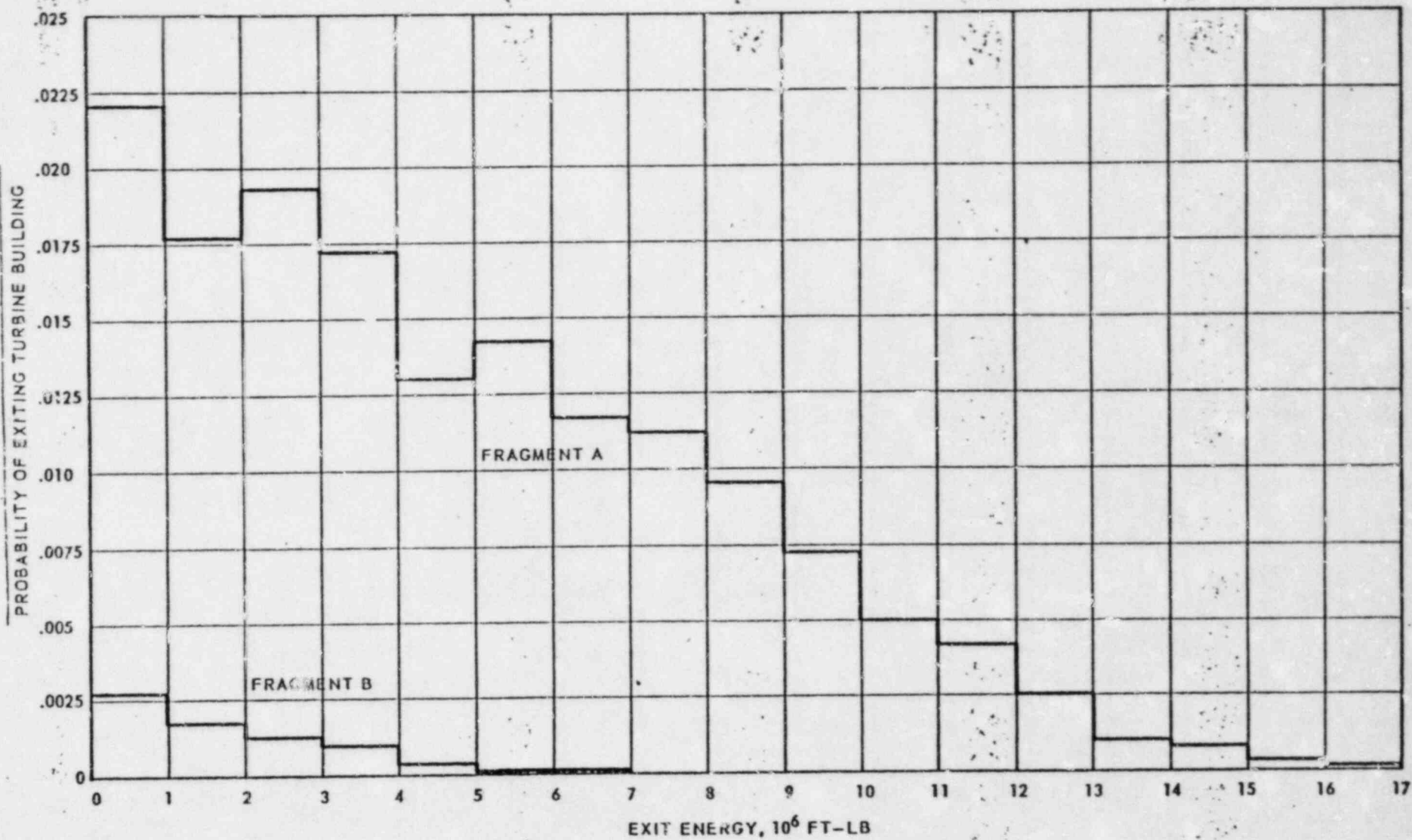


TABLE 3-3

P₃ DAMAGE PROBABILITIES FOR SINGLE IMPACT
DESTRUCTIVE OVERSPEED

(Standard Deviations Appear in Parentheses)

TARGET	WHEEL GROUP I				WHEEL GROUP II				WHEEL GROUP III			
	Fragment				Fragment				Fragment			
	A	B	C	D	A	B	C	D	A	B	C	D
Control Room Elev. 654.5' to 679.5'	0	0	0	0	0	0	0	0	1.33 E-1 (1.9-2)	2.17 E-3 (1.3-3)	0	0
Cable Spreading Room Elev. 647.5' to 654.5'	0	0	0	0	3.20 E-3 (2.2 E-3)	4.64 E-3 (2.7 E-3)	0	0	1.59 E-1 (3.3 E-2)	8.40 E-3 (3.4 E-3)	0	0
HVAC Equipment Room Elev. 654.5' to 702.2'	0	0	0	0	0	0	0	0	1.33 E-1 (1.9 E-2)	2.17 E-3 (1.3 E-3)	0	0
Intermediate Bldg. Elev. 647.5' to 707.5'	0	0	0	0	0	0	0	0	5.26 E-2 (1.9 E-2)	0	0	0
Electrical Penetration Area Elev. 647.5' to 652'	0	0	0	0	0	0	0	0	5.26 E-2 (1.3 E-2)	0	0	0
Auxiliary Building Elev. 647.5 to 652'	0	0	0	0	7.20 E-4 (8.9 E-4)*	0	0	0	1.48 E-1 (3.2 E-2)	5.60 E-3 (2.8 E-3)	0	0
Containment Vessel #1 Below Elev. 706'	0	0	0	0	0	0	0	0	0	0	0	0
Containment Vessel #1 Above Elev. 706'	0	0	0	0	2.70 E-4 (2.1 E-4)	5.33 E-3 (1.7 E-3)	3.10 E-4 (3.1 E-4)*	0	5.52 E-2 (7.3 E-3)	1.78 E-3 (8.7 E-4)	0	0
Containment Vessel #2 Elev. 647.5' to 735'	0	0	0	0	0	0	0	0	0	0	0	0
Containment Vessel #2 Above Elev. 735'	0	0	0	0	0	0	0	0	0	0	0	0

* Fails Shapiro-Wilk Test for Standard Deviation

TABLE 1-4

P₃ DAMAGE PROBABILITIES FOR DOUBLE IMPACT
DESTRUCTIVE OVERSPEED

TARGET	WHEEL GROUP I Impact Configuration				WHEEL GROUP II Impact Configuration				WHEEL GROUP III Impact Configuration						
	AB	AC	BC	AA	AB	AC	BC	AA	AB	AC	BC	AA			
Control Room Elev. 656.5' to 679.5'	5.00 E-4	2.00 E-4	1.00 E-4	0.	0.	2.99 E-2	5.90 E-3	5.80 E-3	8.00 E-4	2.46 E-2	3.14 E-1	2.19 E-1	2.98 E-2	2.60 E-3	6.13 E-1
Cable Spreading Room Elev. 647.5' to 654.5'	3.90 E-3	4.00 E-4	4.00 E-4	0.	2.00 E-3	6.81 E-2	1.50 E-2	2.04 E-2	2.40 E-3	4.42 E-2	3.42 E-1	2.55 E-1	4.96 E-2	2.06 E-2	6.30 E-1
HVAC Equipment Room Elev. 654.5' to 702.2'	5.00 E-4	2.00 E-4	1.00 E-4	0.	0.	2.09 E-2	3.90 E-3	5.80 E-3	8.00 E-4	2.46 E-2	3.14 E-1	2.19 E-1	2.98 E-2	2.60 E-3	6.13 E-1
Intermediate Building Elev. 647.5' to 702.5'	0.	0.	0.	0.	0.	7.00 E-4	1.00 E-4	0.	0.	6.00 E-4	1.91 E-1	1.19 E-1	5.90 E-3	0.	5.00 E-1
Electrical Penetration Area Elev. 647.5' to 654.5'	0.	0.	0.	0.	0.	7.00 E-4	1.00 E-4	0.	0.	6.00 E-4	1.91 E-1	1.19 E-1	5.90 E-3	0.	5.00 E-1
Auxiliary Building Elev. 647.5' to 652.5'	0.	0.	0.	0.	0.	4.72 E-2	7.00 E-3	7.00 E-3	0.	3.32 E-2	3.31 E-1	2.36 E-1	3.83 E-2	9.40 E-3	5.25 E-1
Containment Vessel #1 Below Elev. 706'	0.	0.	0.	0.	0.	1.60 E-3	2.00 E-4	3.00 E-4	0.	1.20 E-3	3.59 E-2	1.62 E-2	4.00 E-4	0.	1.91 E-1
Containment Vessel #1 Above Elev. 706'	1.30 E-3	2.00 E-4	1.00 E-3	0.	2.00 E-4	2.77 E-2	5.90 E-3	1.47 E-2	2.20 E-3	1.50 E-2	1.86 E-1	1.04 E-1	1.79 E-2	6.80 E-3	5.68 E-1
Containment Vessel #2 Elev. 647.5' to 735'	0.	0.	0.	0.	0.	0.	0.	0.	0.	0.	0.	0.	0.	0.	0.
Containment Vessel #2 Above Elev. 735'	0.	0.	0.	0.	0.	1.60 E-3	2.00 E-4	3.00 E-4	0.	1.20 E-3	3.59 E-2	1.62 E-2	4.00 E-4	0.	1.91 E-1

TABLE 3-5

P₃ DAMAGE PROBABILITIES FOR TRIPLE IMPACT

WHEEL GROUP I

<u>TARGET</u>		<u>IMPACT CONFIGURATION</u>					
<u>DESIGN OVERSPEED</u>		A-A-B	A-A-C	A-B-C	B-C-C	A-C-C	C-C-C
Control Room Elev. 654.5' to 679.5'		0	0	0	0	0	0
Containment Vessel #1 Below Elev. 706'		0	0	0	0	0	0
Containment Vessel #1 Above 706'		0	0	0	0	0	0
Containment Vessel #2 Elev. 647.5' to 735'		0	0	0	0	0	0
Containment Vessel #2 Above Elev. 735'		0	0	0	0	0	0
<u>DESTRUCTIVE OVERSPEED</u>							
Control Room Elev. 654.5' to 679.5'		1.40 E-3	1.33 E-3	1.04 E-3	0	0	0
Containment Vessel #1 Below Elev. 706'		6.67 E-5	0	4.00 E-5	0	0	0
Containment Vessel #1 Above Elev. 706'		2.87 E-3	1.37 E-3	2.52 E-3	0	0	0
Containment Vessel #2 Elev. 647.5' to 735'		0	0	0	0	0	0
Containment Vessel #2 Above Elev. 735'		6.67 E-5	0	4.00 E-5	0	0	0

TABLE 3-5 (Cont'd)

WHEEL GROUP II

<u>TARGET</u>	<u>IMPACT CONFIGURATION</u>					
<u>DESIGN OVERSPEED</u>	A-A-B	A-A-C	A-B-C	B-C-C	A-C-C	C-C-C
Control Room Elev. 654.5' to 679.5'	0	6.67 E-5	0	0	0	0
Containment Vessel #1 Below Elev. 706'	0	0	0	0	0	0
Containment Vessel #1 Above 706'	0	0	0	0	0	0
Containment Vessel #2 Elev. 647.5' to 735'	0	0	0	0	0	0
Containment Vessel #2 Above Elev. 735'	0	0	0	0	0	0
<u>DESTRUCTIVE OVERSPEED</u>						
Control Room Elev. 654.5' to 679.5'	9.03 E-2	3.96 E-2	4.59 E-2	1.27 E-2	1.27 E-2	2.0 E-3
Containment Vessel #1 Below Elev. 706'	1.15 E-2	2.67 E-3	5.60 E-3	2.07 E-3	1.07 E-3	2.0 E-4
Containment Vessel #1 Above Elev. 706'	5.75 E-2	2.33 E-2	3.89 E-2	2.57 E-2	1.13 E-2	5.40 E-4
Containment Vessel #2 Elev. 647.5' to 735'	0	0	0	0	0	0
Containment Vessel #2 Above Elev. 735'	1.15 E-2	2.67 E-3	5.60 E-3	2.07 E-3	1.07 E-3	2.0 E-4

TABLE 3-5 (Cont'd)

WHEEL GROUP III

TARGET	IMPACT CONFIGURATION					
DESIGN OVERSPEED	A-A-B	A-A-C	A-B-C	B-C-C	A-C-C	C-C-C
Control Room Elev. 654.5' to 679.5'	1.69 E-2	1.21 E-2	3.60 E-3	0	1.7 E-3	0
Containment Vessel #1 Below Elev. 706'	2.67 E-4	0	1.20 E-4	0	0	0
Containment Vessel #1 Above Elev. 706'	6.67 E-4	8.67 E-4	1.60 E-4	0	6.67 E-5	0
Containment Vessel #2 Elev. 647.5' to 735'	0	0	0	0	0	0
Containment Vessel #2 Above Elev. 735'	2.67 E-4	0	1.20 E-4	0	0	0
DESTRUCTIVE OVERSPEED						
Control Room Elev. 654.5' to 679.5'	6.94 E-1	6.53 E-1	3.99 E-1	6.68 E-2	2.95 E-1	1.66 E-2
Containment Vessel #1 Below Elev. 706'	3.38 E-1	2.70 E-1	7.96 E-2	6.70 E-3	4.50 E-2	2.40 E-3
Containment Vessel #1 Above Elev. 706'	6.27 E-1	5.93 E-1	2.36 E-1	3.67 E-2	1.61 E-1	1.68 E-2
Containment Vessel #2 Elev. 647.5' to 735'	0	0	0	0	0	0
Containment Vessel #2 Above Elev. 735'	3.38 E-1	2.70 E-1	7.96 E-2	6.70 E-3	4.50 E-2	2.04 E-3

3.5 TARGET DAMAGE PROBABILITIES - P_4

Overall P_4 damage probabilities are evaluated by considering the probability of missile impact and the conditional probability of damage based on a given impact configuration. In evaluating probabilities mutually exclusive sets of events are considered for single, double, and triple impacts. The total damage estimate is calculated as the sum of the damage probabilities calculated for each of the three impact configuration sets. Higher order configurations can be neglected as discussed in Section 3.4.5. A total of 41 impact combinations per wheel group are evaluated for each target-missile generation site pairing.

Calculated P_4 values for all targets within the LTM zone appear in Table 3-6. As noted in Section 3.0, only the risk associated with Unit 1 turbines is presented in this table. Based on symmetry arguments the Unit 2 turbines have similar risk values.

When evaluating all targets, triple impact P_3 values are assumed to be equal to the Control Room values given in Table 3-5 because of the relatively small effect on the P_4 probability. The exception is evaluation of the Containment Vessel targets. This procedure is conservative, yet demonstrates the relative magnitude of the hazard.

TABLE 3-6

TURBINE MISSILE HAZARD TO LTM TARGETS

 P_4 ANNUAL PROBABILITY OF DAMAGE

<u>TARGET</u>	<u>SINGLE STRIKE IMPACTS</u>	<u>DOUBLE STRIKE IMPACTS</u>	<u>TRIPLE STRIKE IMPACTS</u>	<u>TOTAL</u>
Control Room Elev. 654.5' to 679.5'	1.3 E-8	2.0 E-9	7.8 E-11	1.5 E-8
Cable Spreading Room Elev. 647.5' to 654.5'	5.2 E-9	2.3 E-10	1.9 E-12	5.4 E-9
HVAC Equipment Room Elev. 654.5' to 702.2'	1.4 E-8	2.4 E-9	1.0 E-10	1.7 E-8
Intermediate Building Elev. 647.5 to 707.5'	5.5 E-9	2.2 E-9	5.5 E-10	8.2 E-9
Electrical Penetration Area Elev. 647.5' to 654'	7.0 E-10	2.7 E-11	1.4 E-12	7.3 E-10
Auxiliary Building Elev. 647.5' to 652'	5.4 E-9	2.9 E-10	4.8 E-12	5.7 E-9
Containment Vessel #1 Elev. 647.5' to 750'	7.0 E-9	4.1 E-9	8.5 E-10	1.2 E-8
Containment Vessel #2 Elev. 647.5' to 750'	0	2.0 E-12	2.1 E-14	2.0 E-12

3.6 CONCLUSION

The turbine missile hazard to an individual safety related target has been conservatively demonstrated to be less than 1.5 E-8 per year per turbine. This acceptably low value is within the limits prescribed in Regulatory Guide 1.115 and, therefore, redesign for additional turbine missile protection is unnecessary.

REFERENCES

1. Preliminary Safety Analysis Report, Perry Nuclear Power Plant. Docket Nos. 50-440/441, Cleveland Electric Illuminating Co., Cleveland, Ohio.
2. Gonyea, D. C., "An Analysis of the Energy of Hypothetical Wheel Missiles Escaping From Turbine Casings", DF73LS12, General Electric Co., February 1973.
3. Bush, S. H., "Probability of Damage to Nuclear Components Due to Turbine Failure", Nuclear Safety, Vol. 14, No. 3, May-June 1973.
4. Memo Report, "Hypothetical Turbine Missiles - Detailed Sample Calculations", General Electric Co., 12/1/73.
5. Hagg, A. C. and Sankey, G. O., "The Containment of Disc Burst Fragments by Cylindrical Shells", Paper No. 73-WA-PWR-2, ASME Winter Meeting, Detroit, Michigan, November 11-15, 1973.
6. Linderman, R. B. et al, "Design of Structures for Missile Impact", BC-TOP-2, Revision 2, Bechtel Power Corporation, September 1974.
7. Amirikan, A., "Design of Protective Structures (A New Concept of Structural Behavior)", NAVDOCKS P-51, Annual Meeting of ASCE, October 1950.
8. Williamson, R. A., and Alvy, R. R., "Impact Effect of Fragments Striking Structural Elements", Holmes & Narver, Inc., Revised November 1973.
9. Johnson, B. et al, "Analysis of the Turbine Missile Hazard to the Nuclear Thermal Power Plant at Pebble Springs, Oregon", Docket Nos. 50-514, Portland General Electric Co., Portland, Oregon.

REFERENCES (Cont'd)

10. Shapiro, S. and Wilk, M. B., "An Analysis of Variance Test for Normality (Complete Samples)", *Biometrika*, Vol. 52, P. 591, 1965.
11. Burrows, G. L., and MacMillian, "Confidence Limits for Monte Carlo Calculations", *Nuc. Sci. and Eng.*, Vol. 22, p. 384, 1965.

APPENDIX A

/ RESIDUAL PERFORATION VELOCITY

Appendix A

Residual Perforation Velocity

The Ballistic Research Laboratories (BRL) formulae for concrete and steel are two commonly used methods for evaluating perforation of barriers. A comparison is made between the residual velocities through barriers as calculated by the methods used in Section 3.4.2 and those predicted by use of the BRL equations.

A.1 Residual Velocity in Concrete

The BRL formula for perforation of a 3000 psi reinforced concrete slab of thickness T is (1)

$$T = 7.8 \frac{W D^{0.2}}{D^2} \left(\frac{V}{1000} \right)^{1.33} \quad (A-1)$$

where

D = diameter of missile, in.

T = thickness of concrete slab that will be perforated, in.

W = missile weight, lb.

V = impact velocity, fps.

Using the criterion appearing in Equation (8) of Section 3.4.2, the BRL residual velocity v_r after perforation of a barrier of thickness T is

$$v_r = \sqrt{v_i^2 - \left[\frac{TD^{1.8}}{7.8 W} \right]^{1.5}} \quad (A-2)$$

where

v_r = residual velocity, fps.

v_i = impact velocity, fps.

T = barrier thickness, in.

W = missile weight, lb.

D = diameter of missile, in.

For irregularly shaped missiles of impact area A, an equivalent cylindrical diameter of

$$D = \sqrt{\frac{4A}{\pi}} \quad (A-3)$$

is used.

The residual velocity of perforation as calculated in this study is based on the modified Petry formula, and is given in Section 3.4.2.2.2 by

$$v_r = \sqrt{v_i^2 - 215000 \left[10^{T/(2KA_p)} - 1 \right]} \quad (A-4)$$

A comparison of Equations A-2 and A-4 is presented in Figures A-1 to A-3 for minimum area Wheel Group III missiles over arbitrary impact velocity ranges.

Little difference exists between the predictions of both methods.

A.2 Residual Velocity in Steel

The BRL formula for perforation of a steel plate of thickness T is ⁽¹⁾

$$T^{1.5} = \frac{0.5 \cdot MV^2}{17,400 K^2 D^{1.5}} \quad (A-5)$$

where

T = steel wall thickness, in.

M = mass of the missile, lb-sec²/ft.

V = velocity of missile, fps.

K = empirical constant usually assumed as 1.0.

D = diameter of missile, in.

For irregularly shaped missiles, Equation (A-3) is used to calculate an effective diameter for use with Equation (A-5).

Again, using the criterion in Section 3.4.2, the residual velocity after perforation of a barrier based on the BRL formula in Equation (A-5) is

$$v_r = \left[v_i^2 - \frac{(1.12 \text{ E}+6)(DT)^{1.5}}{W} \right]^{1/2} \quad (\text{A-6})$$

where

v_i = incident missile velocity, fps.

v_r = residual velocity, fps.

D = missile diameter, in.

T = barrier thickness, in.

W = missile weight, lb.

A comparison of the residual velocities predicted by Equation (A-5) and the Hagg-Sankey method as given in Section 3.4.2.1 for minimum area Wheel Group III missiles appears in Figures A-4 to A-6. Discontinuities exist in the Hagg-Sankey results as previously discussed in Section 3.4.2.1.

Over the velocity range of concern, the Hagg-Sankey method predicts larger residual velocities than the BRL formulation. The Hagg-Sankey method is considered to be more accurate for the lower velocity, larger mass, blunt missiles. At very great velocities better agreement exists between both models.

(1) Gwaltney, R.C., Missile Generation and Protection in Light-Water-Cooled Power Reactor Plants, ORNL-NSIC-22, September 1968.

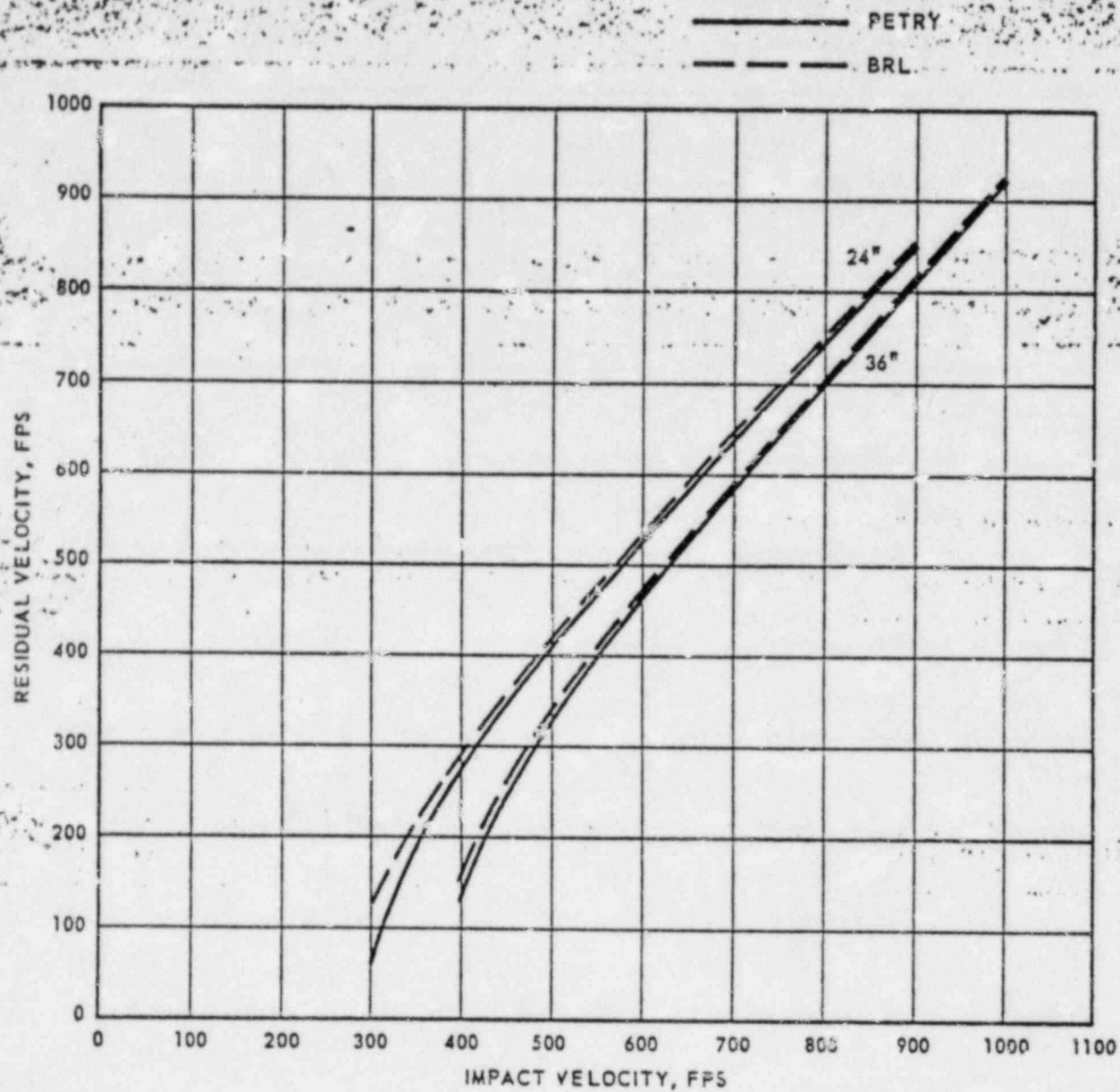


FIGURE A-1
RESIDUAL PERFORATION VELOCITIES
FOR WHEEL GROUP III, FRAGMENT A
THROUGH 3000 PSI CONCRETE

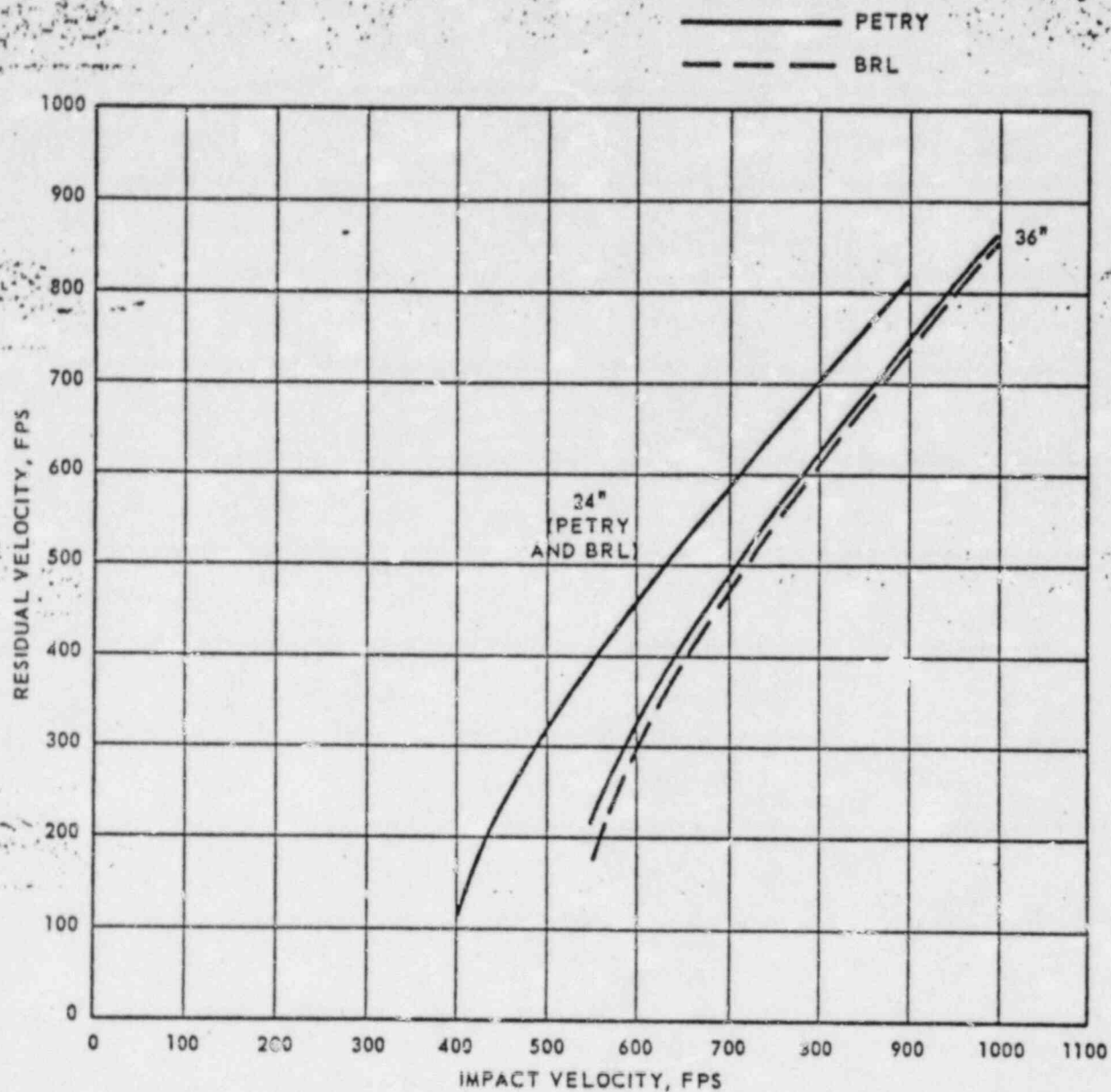


FIGURE A-2
RESIDUAL PERFORATION VELOCITIES
FOR WHEEL GROUP III, FRAGMENT B
THROUGH 3000 PSI CONCRETE

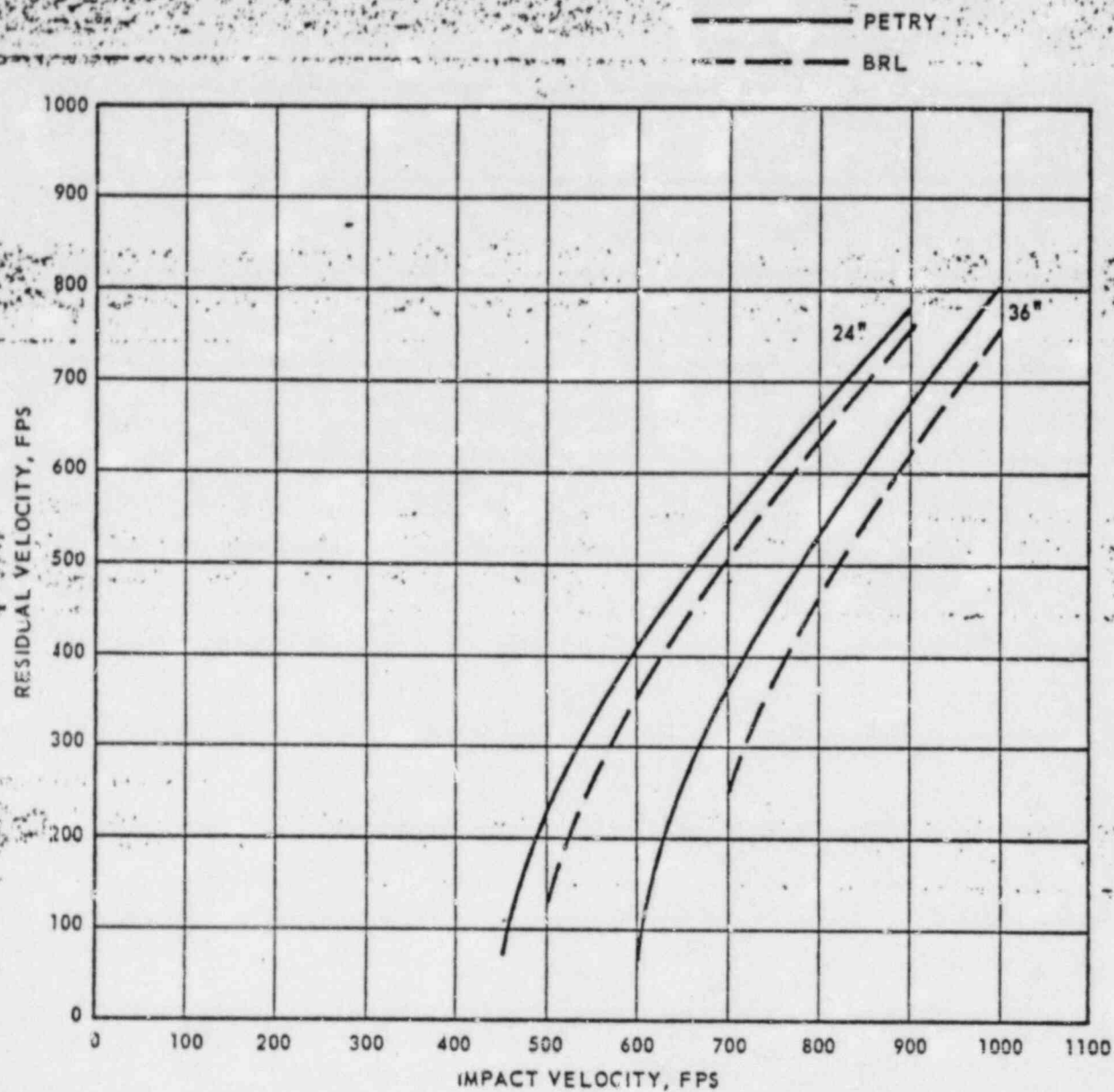


FIGURE A-3
RESIDUAL PERFORATION VELOCITIES
FOR WHEEL GROUP III, FRAGMENT C
THROUGH 3000 PSI CONCRETE

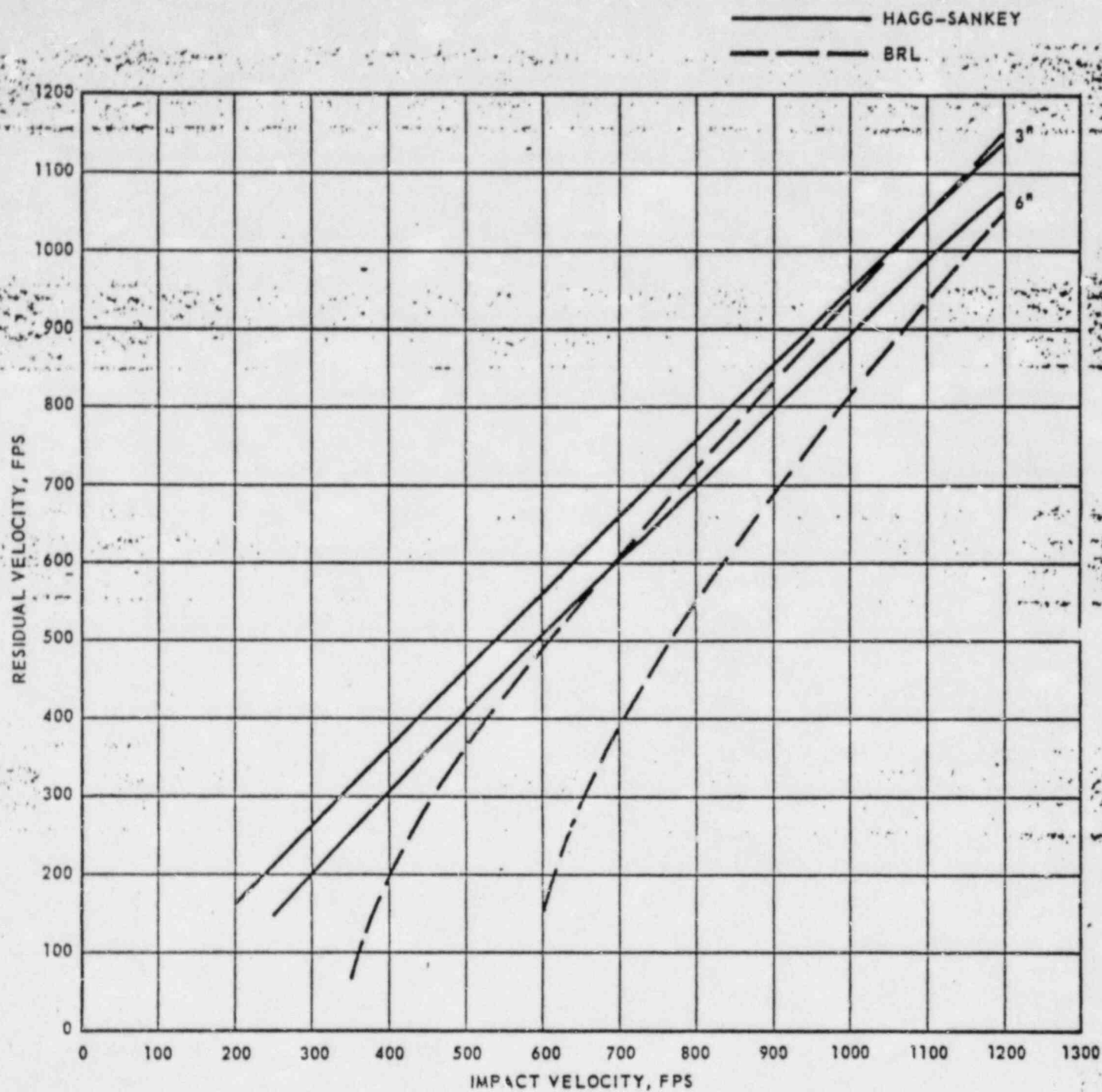


FIGURE A-4
RESIDUAL PERFORATION VELOCITIES
FOR WHEEL GROUP III, FRAGMENT A
THROUGH A-36 STEEL

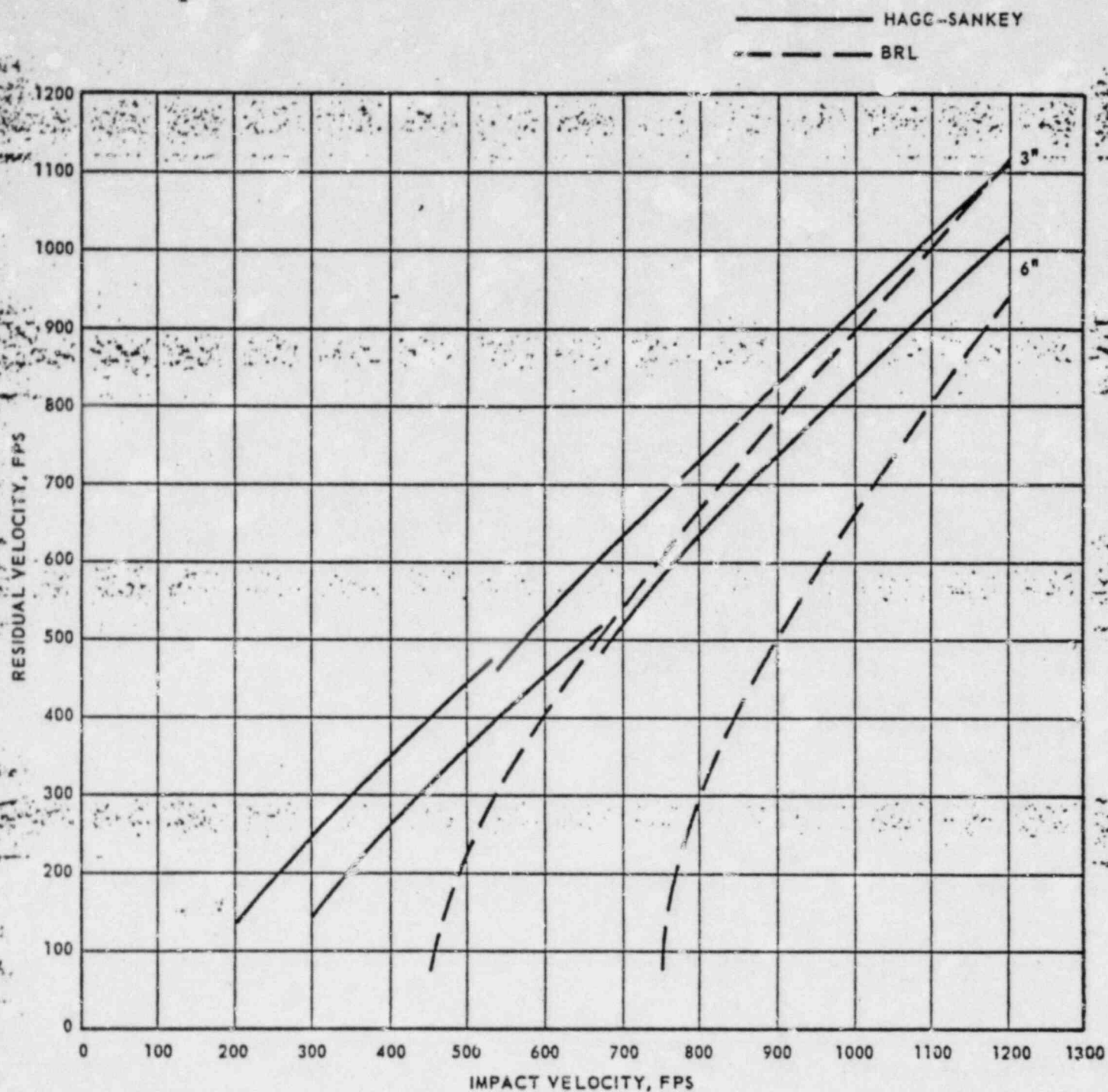


FIGURE A-5
RESIDUAL PERFORATION VELOCITIES
FOR WHEEL GROUP III, FRAGMENT B
THROUGH A-36 STEEL

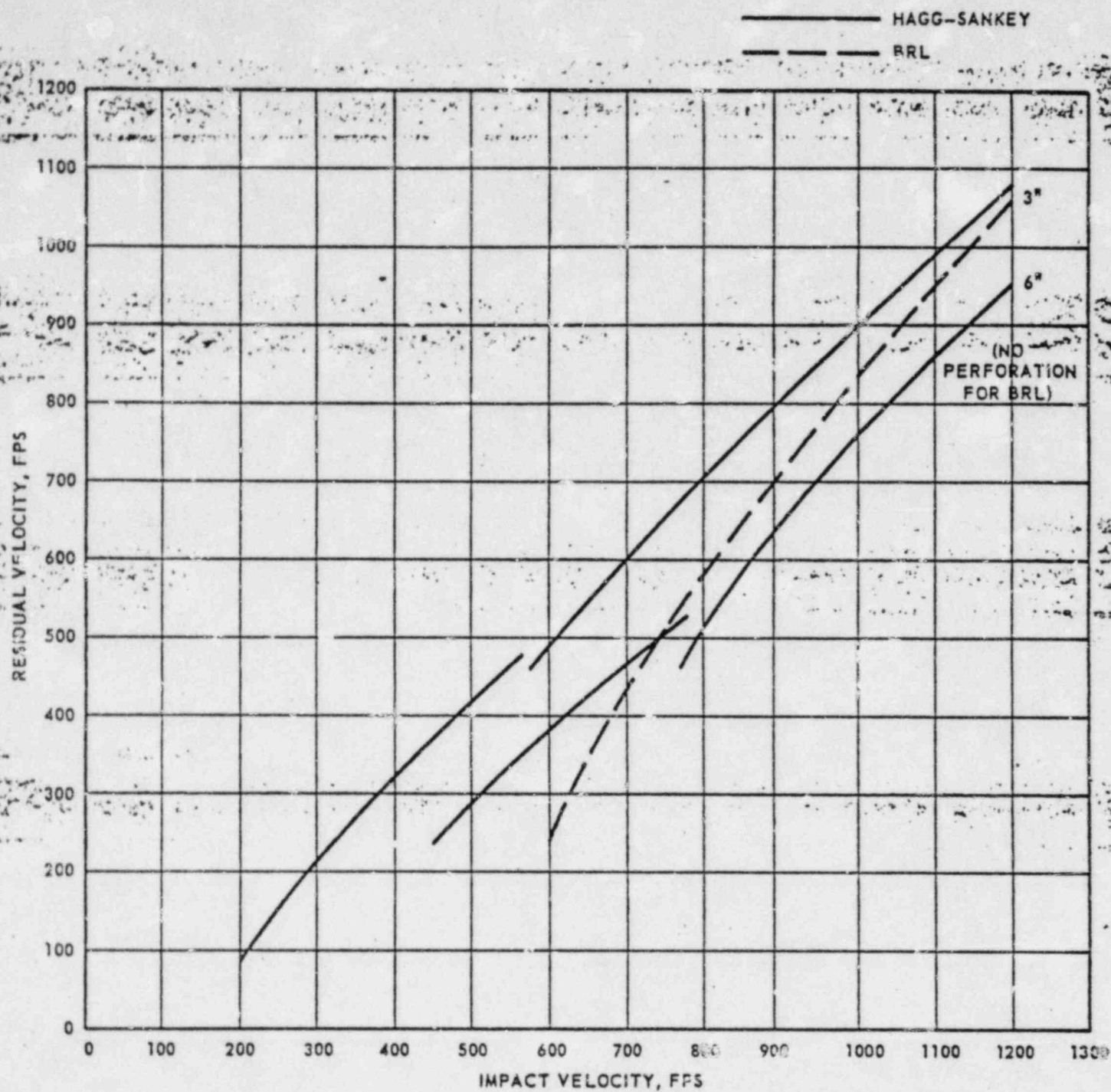


FIGURE A-6
RESIDUAL PERFORATION VELOCITIES
FOR WHEEL GROUP III, FRAGMENT C
THROUGH A-36 STEEL